AD-A080 801 NORTON CO WORCESTER MASS INDUSTRIAL CERAMICS DIV F/G 13/8
SEVERE ENVIRONMENT TESTING OF SILICON NITRIDE ROLLING ELEMENTS.--ETC(U)
NOV 79 J W LUCEK, L B SIBLEY, J W ROSENLIEB N00019-77-C-0551
UNCLASSIFIED NL

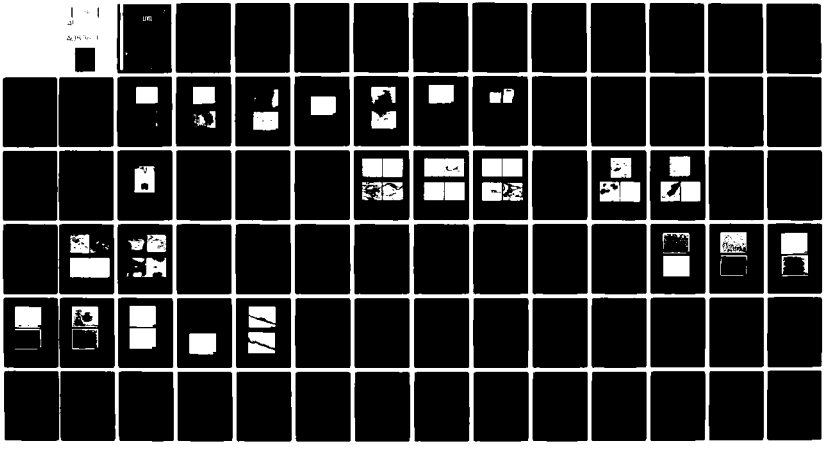

END
DATE FILMED
3-80
DDC

UNCLASSIFIED

SECURITY CLASSIFICATION OF THIS PAGE (When Data Entered)

REPORT DOCUMENTATION PAGE	READ INSTRUCTIONS BEFORE COMPLETING FORM
1. REPORT NUMBER	2. GOVT ACCESSION NO. / 3. RECIPIENT'S CATALOG NUMBER (9)
4. TITLE (and Subtitle) (6) SEVERE ENVIRONMENT TESTING OF SILICON NITRIDE ROLLING ELEMENTS	5. TYPE OF REPORT & PERIOD COVERED FINAL rept. 30 DEC 77 — 2MAR 79 / 6. PERFORMING ORG. REPORT NUMBER
7. AUTHOR(s) (10) John W. Lucek (Norton Company) Worcester, MA 01606; L. B. Sibley and J. W. Rosenlieb SKF Industries, INC. King of Prussia, PA	8. CONTRACT OR GRANT NUMBER(s) (15) N00019-77-C-0551
9. PERFORMING ORGANIZATION NAME AND ADDRESS Norton Company Industrial Ceramics Division / Worcester, MA 01606	10. PROGRAM ELEMENT, PROJECT, TASK AREA & WORK UNIT NUMBERS
11. CONTROLLING OFFICE NAME AND ADDRESS (11) Department of the Navy Naval Air Systems Command Washington, DC 20360	12. REPORT DATE NOVEMBER 1979 / 13. NUMBER OF PAGES 83
14. MONITORING AGENCY NAME & ADDRESS (if different from Controlling Office) DCASR 666 Summer Street (12) 85 Boston, MA 02210	15. SECURITY CLASS. (of this report) Unclassified / 15a. DECLASSIFICATION/DOWNGRADING SCHEDULE

16. DISTRIBUTION STATEMENT (of this Report)

Approved for public release; distribution unlimited.

17. DISTRIBUTION STATEMENT (of the abstract entered in Block 20, if different from Report)

18. SUPPLEMENTARY NOTES

19. KEY WORDS (Continue on reverse side if necessary and identify by block number)

Rolling Contact Bearings
Silicon Nitride
Dry Film Lubrication
High Temperature
Wear Testing
Hertzian Contact

20. ABSTRACT (Continue on reverse side if necessary and identify by block number)

Wear rates for dry film lubricated rolling-spinning contacts of silicon nitride surfaces were studied to 540°C wear rate was essentially constant to 315°C. Surface stress modifications in hot pressed silicon nitride have been shown to improve tensile stress behavior under high magnitude Hertzian stress fields.

DD FORM 1 JAN 73 1473 EDITION OF 1 NOV 65 IS OBSOLETE

UNCLASSIFIED

SECURITY CLASSIFICATION OF THIS PAGE (When Data Entered)

408 070

SUMMARY

Hot pressed silicon nitride has the potential to operate in both thermal and corrosive bearing environments beyond the range of currently available bearing steels and liquid hydrocarbon lubricants. Dry film lubricated contacts of silicon nitride were studied in a rolling four ball tester up to 540°C (1000°F) at contact stresses of 2.8 GN/m^2 (400 KSI). It was found that dry rolling-spinning contacts of silicon nitride surfaces under heavy load at ambient temperatures exhibit the same magnitude wear coefficient as boundary lubricated bearing steels studied previously. This is felt to represent a major improvement over the performance of "dry" steel contacts at high temperatures. The wear rate of these dry contacts does not significantly increase to temperatures of 315°C (600°F). Above that temperature the testing results are unreliable due to insufficient data and complications from cage material oxidation and interaction with the AISI M-1 steel support cup.

Data indicates that limited life application of dry silicon nitride contacts at high loads is feasible; but is too limited at this point to design high temperature bearings. No clear improvement in wear behavior was noted with the incorporation of dry film lubrication coatings on wear surfaces; potential still exists for long life, high temperature application of silicon nitride bearings at lower loads or with copious supply dry film lubrication.

Chemical tempering of silicon nitride surfaces was not demonstrated to increase measured material strength. Oxidation of machined surfaces was shown to increase the tensile stress required to fracture the material in Hertzian loading but also degraded the compressive strength of the surface. A reduced integrity under high magnitude cyclic compressive loads, as encountered in bearings, will result in increased wear and loss of geometry. Oxidation of silicon nitride surfaces must be modified to retain the compressive capabilities of the material. Techniques for machining and characterization of near net shape NC-132 silicon nitride blanks have been developed.

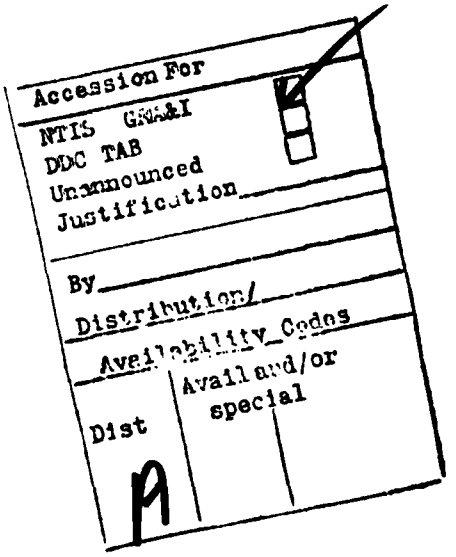

FOREWORD

This report describes efforts carried out under Naval Air Systems Command contract NASC N00019-77-C-0551 for the period 30 December 1977 through 2 March 1979. The objective was to study the behavior of silicon nitride rolling contacts in severe; high temperature, dry film lubricated conditions.

This program was designed by personnel of both Norton Company, Worcester, MA and SKF Industries, King of Prussia, PA. Principal investigator at the Norton Company was Mr. J. W. Lucek. The rolling contact testing and analysis portion of the program was carried out by SKF Industries. Mr. H. M. Dalal (now of KSM Fastening Systems) and Mr. L. B. Sibley were principal investigators at SKF.

The authors wish to thank the sponsoring Navy Department, Naval Air Systems Command, for the opportunity to study and clarify the behavior of silicon nitride ceramics in severe environments, as well as the research support groups at both Norton Company and SKF Industries for their assistance in this program.

TABLE OF CONTENTS

LIST OF TABLES

LIST OF FIGURES

LIST OF FIGURES (continued)

I. INTRODUCTION

Hot pressed silicon nitride materials have demonstrated a potential for use in rolling contact bearings where the environment exceeds the capabilities of currently available bearing steels. The material's unique properties include; noncatastrophic (spalling) failure in the rolling contact environment, purely elastic response to structural magnitude strains up to temperatures of 1000°C (1800°F), and almost complete chemical inactivity up to 700°C (1300°F). Long term study of the material (See Appendix C) has shown it to be useful in rolling contact environments with liquid lubrication films. The completed program describes the first major effort to capitalize on the high temperature capabilities of the silicon nitride material in a dry film lubricated, high contact stress, rolling contact bearing environment.

One bearing application where high magnitude loads must be carried at elevated temperatures is the angular contact ball thrust bearing in the small, limited life turbine engine for cruise missile or target drone power plants. Currently, a complicated cooling system is used to maintain bearing temperatures in the range where metallic materials are useful. Substitution of a bearing with less response to high temperatures could reduce the engines dependance on cooling systems; decreasing weight and increasing reliability. The use of all-silicon nitride roller bearings in a small, limited life turbine shaft bearing with no lubrication has already been successfully demonstrated.[1] The thrust bearing of such an engine constitutes a slightly less severe thermal environment but is under constant, heavy load and constitutes the basic environment studied in this program. Testing was done at 2.8 GN/m^2 (400 KSI) maximum contact stress, at 10K rpm, and up to temperatures of 540°C (1000°F). Both sputter-coated and glass bonded graphite and molybdenum disulfide lubricants were studied in a rolling four-ball tester. The wear coefficient and mode were studied for each lubricating system.

The principle failure mode of ceramic materials is under tensile stress. Silicon nitride materials are theoretically amenable to a chemical "tempering" process whereby the loads required to cause tensile failure are increased. Surface oxidation can also increase the stress necessary to induce fracture by blunting surface flaws. Ceramic materials fail in tension in Hertzian stress fields: the above mechanisms were studies as a means of improving the performance of silicon nitride in the rolling contact environment.

This program was also the first to use NC-132 silicon nitride pressed to near net shape (NNS) in large (>200) quantities. This production process eliminates considerable rough machining and material wastage. Specialized qualification

procedures were developed to assure the quality of the silicon nitride forms produced. Ultrasonic machining techniques were used to rough the blanks to a suitable geometry for ball grinding. Tumbling was also studied as a method of roughing the as-pressed blanks to a spherical geometry.

II. SPECIMEN PRODUCTION

A. Material Manufacture

Until recently, dense silicon nitride materials suitable for rolling contact environments have been available only in the form of large billets. Individual test or bearing components were diamond machined from billet stock resulting in material waste and high machining costs. Recent efforts to produce NC-132 near net shape (NNS) elements have shown that small blanks from multiple cavity dies can possess the same wear and fatigue properties of NC-132 silicon nitride billet material.[2] Characterization of NNS NC-132 silicon nitride blanks had indicated that density, inclusion content, porosity, and the attendant mechanical properties were unaffected.[2]

Because of these developments and the potential reduction of machining costs this program, originally planned using silicon nitride billet material, was modified to use near net shape (NNS) material. This program sampled the first, large quantity (>200 elements) pressing of NC-132 hot pressed silicon nitride. During the production run, a smaller than expected die wall-element reaction occurred and resulted in cylindrical blanks approximately 5 mm (0.2 in.) oversize in length. Of the 243 elements, 210 passed inspection at Norton and were sliced to length prior to shipment for ball processing at SKF. Qualification of the material is discussed in a following section. Characteristics of the as-pressed elements are presented in Table A.

TABLE A

Characteristics of NC-132 Si_3N_4 Elements

	Light Sandblast	Heavy Sandblast
Outside Diameter		
mean	15.11 mm (0.595")	14.71 mm (0.579")
σ	0.20 mm (0.008")	0.13 mm (0.005")
n	12	9
Height		
mean	22.17 mm (0.873")	21.67 mm (0.853")
σ	0.48 mm (0.019")	0.56 mm (0.022")
n	12	9
Immersion Density		
average		3.23 g/cc
standard deviation		0.03
n		43*

*mean calculated on 12 clean specimens, σ on 43 lightly sandblasted

The program also planned study of the rolling contact behavior of NCX-34 Si_3N_4-Y_2O_3 hot pressed material. Characterization of this material indicates that it is stronger than NC-132 and that its fracture energy is similar and possibly higher.[3,4] The attempt to press this material to shape was made unsuccessfully due to a higher than anticipated powder-die cavity interaction. The geometry of the mold cavities was destroyed in this pressing attempt and no further runs were made. A rearrangement of the testing schedule compensated for the loss of this material in terms of research effort to be expended.

B. Material Qualification

1. General - NC-132 hot-pressed silicon nitride is normally qualified with respect to standards on density, radiographic uniformity, chemical impurity analysis, and 4-point modulus of rupture (MOR). The element blanks provided as stock for this program were too small to yield useful MOR specimens; thus, direct comparison with existing modulus of rupture qualification data was not possible. A compressive strength characterization based on ASM Standard C773-74 was substituted.

The element blanks were pressed from NC-132 grade α-silicon nitride powder and exceeded minimum density, chemical, and radiographic uniformity specifications. In order to obtain compressive strength data on NC-132, ASTM C773-74 was modified to allow testing of very strong materials. The modifications are presented in Appendix A. Because no compressive strength data existed for either billet or NNS elements, a fully qualified billet was characterized for uniaxial failure stress to provide a comparison standard for the NNS elements. A summary of the data appears in Table B.

A Student's "t" statistic analysis indicates a highly significant measured experimental strength difference that has been attributed to the geometry of the test specimens. Because of the large (for a ceramic) strain present at failure inaccuracies in geometry can greatly influence compressive strength results. The NNS element specimens had loading faces flat and parallel within an average 0.0025 mm total indicated reading (TIR). The same characteristic for the billet samples was 0.0046 mm TIR; resulting in higher local stresses in the billet material at the same applied load. Since the two material samples exhibited similar strength and the billet material was qualified NC-132 silicon nitride; the NNS elements also were judged to be "typical" strength NC-132.

It is of note that theoretical estimates place the minimum compressive strength of dense silicon nitride materials in the range of 4.1 GN/m^2 (600 KSI). The geometry effect noted above as well as testing technique reduce the anticipated measured

TABLE B

NC-132 Si_3N_4 Qualification
Data Summary

	Specification	Comparison Billet #42775	Element Blanks
Density (g/cc)	>3.21	3.23	3.23
Strength			
Bending MN/m^2 (KSI)			
Mean MOR	>750 (110)	804 (117)	not measured
Std. Dev.		106 (15.4)	
$\bar{X}$ -2σ	>550 (80)	592 (85.9)	
n	≥8	11	
Compression GN/m^2 (KSI)			
Mean σ max	no specification	2.94 (432)	3.27 (474)
Std. Dev.		0.124 (18)	0.172 (25)
$\bar{X}$ -2σ		2.73 (396)	2.92 (424)
n		6	6

failure stress. The loading platens (tungsten carbide) are of larger diameter than the specimen and, under test, deform to increase the strain in the cylindrical speciman surface above the average bulk strain. The strengths reported are thus a complex function of specimen geometry, testing technique, as well as material integrity. Uniformity of variables such as press geometry can effect a major change in the measured compressive strengths.

Further modifications of the compression testing technique may allow resolution of the theoretical material strength. Use of bearing design criteria to design either the platen or test specimen can potentially eliminate the compressive stress inhomogeneity currently obtained. Substitution of a positive curvature crowned surface for either the flat platen or specimen face should negate the effects of the Young's modulii mismatch and distortion of the platen under load. Large radius "spherical" surfaces on the specimen ends are, though difficult to produce, more attractive than crowning the platen as the platens must be resurfaced after each test because of explosive failure. Theoretical and experimental studies will be necessary to define the geometric parameters. Such a study will result in the ability to test the NC-132 material in true uniaxial compression and may shed light on its behavior at or near its failure stress under controlled conditions.

2. Optical - A detailed microstructural evaluation was carried out on the near-net-shape silicon nitride material. Both thin section (~5μm thickness) and metallographic techniques were used. All samples were taken parallel to the flat faces of the cylinders. The thin sections do reveal qualitative information on grain size; but the section thickness was greater than the typical grain size. Thus, confused light paths resulted and little quantitative information could be derived. See Figures 1 and 2. The large dark areas in the micrographs, are of unknown origin as they do not appear to be part of the silicon nitride matrix, but physical contaminants from the polishing sequence.

A suitable metallographic (reflected light) polishing sequence has recently been developed that provides specimens in which individual phases can be identified. Figures 3 and 5 compare the billet and NNS silicon nitride material from the program at 240 magnifications; Figures 4 and 6 at 600X. In Figures 4 and 6, it can be seen that both NC-132 materials exhibit similar phase distributions from content, distribution, and size standpoints. The dark gray dispersed phase is silicon-oxynitride (Si_2ON_2), the light gray dispersed phase is α-Si_3N_4; the dispersed bright phase is probably metallic contaminants; and the medium gray matrix is β-Si_3N_4. The largest grains visible, Si_2ON_2, have apparent diameters of 2-3 μm.

The lower magnification photographs exhibit additional information under crossed nicols. NC-132 silicon nitride is semitransparent in polarized light; that is light which vibrates in the privileged direction of the polarizer. When a second polarizing element is inserted in the light beam reflected from the sample with its privileged direction 90° opposed to that of the source, the field should go nearly extinct (black) as no light should pass the second (analyzer) element. Because when polarized light enters a silicon nitride sample its orientation is slightly changed: complete extinction rarely occurs. It is clear from Figures 3 and 5 that some areas of the materials reorient the polarized light considerably more than others, resulting in "light" areas.

Based on experience gained from less dense silicon nitride materials with similar phase distribution; these light areas, which occur in both billet and NNS NC-132, are felt to indicate lower density areas on a very fine scale. The magnitude of the density difference is currently uncertain; but it has been observed as being related to both porosity and inclusions. This analysis technique should be pursued in future programs.

3. Microhardness - Previous work has indicated that NNS NC-132 elements exhibit a similar microstructural hardness to billet material;[2] both materials in the range of 1400-1600 Kg/mm^2 at a 500 gram indenter load. On the material pressed for

Transmitted polarized light 45X

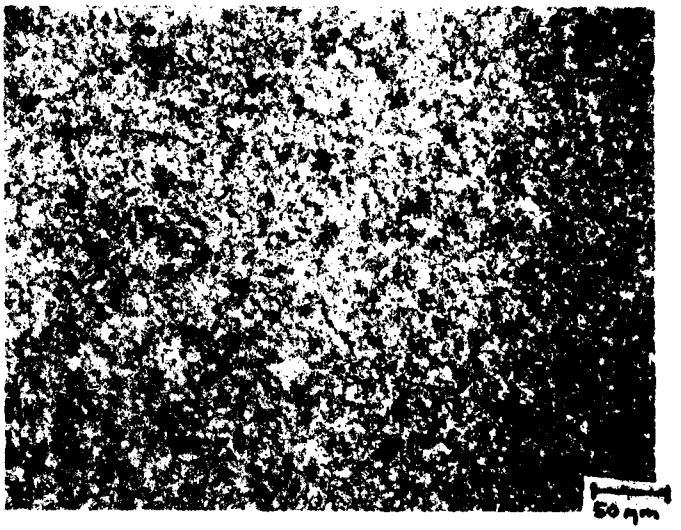

Transmitted polarized light 225X

FIGURE 1 - NC-132 silicon nitride thin section

Transmitted polarized light 450X

Reflected polarized light 450X

FIGURE 2 - NC-132 silicon nitride thin section dark inclusion.

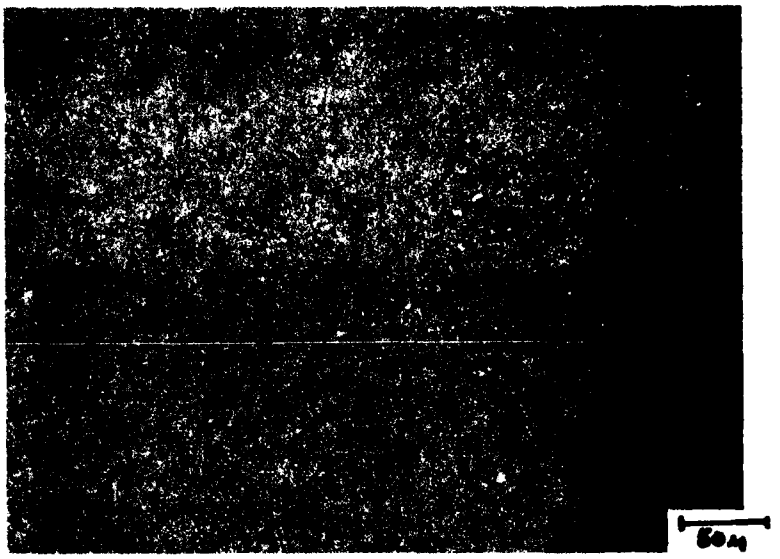

Plane-polarized light 240X

Crossed Nicols 240X

FIGURE 3 - Pressed to shape NC-132 silicon nitride
Reflected light.

Plane polarized light 600X

FIGURE 4 - Pressed to shape NC-132 silicon nitride
polarized light.

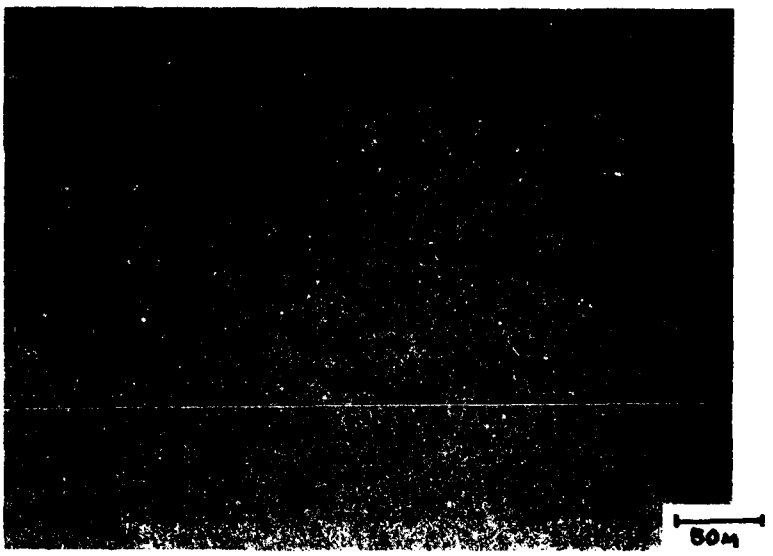

Plane polarized light 240X

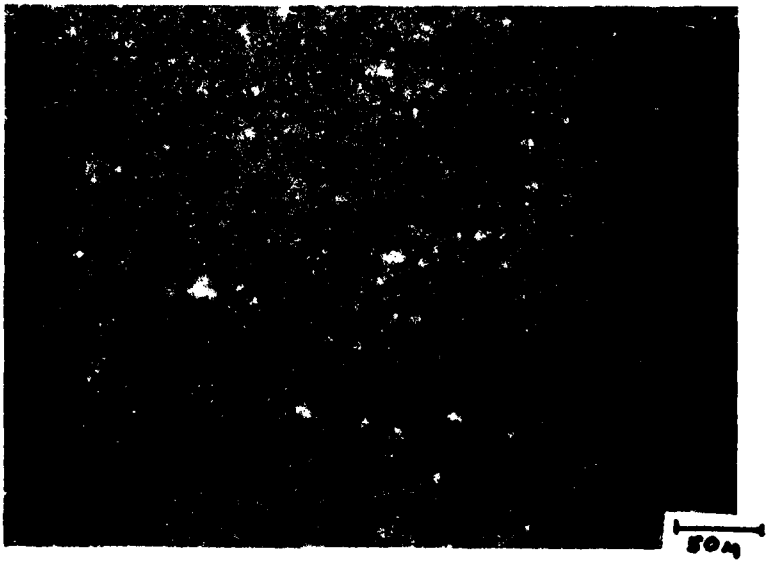

Crossed Nicols 240X

FIGURE 5 - NC-132 silicon nitride billet material
Reflected light.

FIGURE 6 - NC-132 billet material reflected plane polarized light 600X

this program, data obtained at SKF Industries ranged from 1400 to 1500 KG/mm^2 agreed closely with that obtained at Norton 1325-1500 KHN.

C. Test Element Production

1. Tumbling - The qualified hot pressed silicon nitride cylinders were initially tumbled in boron carbide abrasive in an attempt to reduce the blanks to a near spherical shape suitable for direct ball grinding without resorting to controlled machining techniques. The resulting blanks exhibited uneven material removal rates as a function of length. See Figure 7. This behavior is due to a difference in material properties at each end of the cylinder originating from the slicing operation performed earlier. The end of the blank with the greater material removal had a thicker reaction zone on the corner from pressing, while the other end terminated in a "pure" NC-132 silicon nitride surface with considerably higher hardness.

It can be seen that the as-pressed end of the cylinder is approaching a spherical radius; indicating that a uniformly hard blank, i.e. as-pressed surfaces all over, may tumble to a rough sphere given enough processing time. Past efforts on tumbling billet material, however, showed that the material removal rate (MRR) of NC-132 silicon nitride was very low unless the tumbling conditions were made so severe that occasional unacceptable

FIGURE 7 - Uneven tumbling wear on sliced NC-132 blanks.

impact damage occured. For this reason, alternative processes were developed for rough shaping of pressed cylinders into spheres, having more consistent control of process parameters than tumbling.

2. Ultrasonic Machining - The cylindrical blanks were machined ultrasonically to rough spheres prior to groove grinding and lapping, using previously developed procedures.[2] The hot pressed cylinders first were machined into rough spheres using hemispherical cavity tools with light loads (3-5 N/cavity), 320 mesh boron carbide abrasive and a 20,000 Hz ultrasonic transducer, producing an MRR somewhat over 1 cc/hr. These rough spheres were then processed to obtain a truer spherical shape in the same ultrasonic machine, about ten at a time, using toroidal grooved tools at higher loads (20 N/ball), for MRR of about 2 cc/hr.

3. Grinding and Lapping - The ultrasonically machined spheres were then rough ground and finish lapped into ball specimens using standard ball manufacturing machines and processes essentially the same as those described previously.[5,22] The finished balls had a surface roughness (0.05-0.06 mm AA) comparable to the best composite roughness of the contacts obtainable in all silicon nitride ball and roller bearings, but not as low (<0.02 mm AA) as normally obtained on finished aircraft-quality silicon nitride balls.[5] As noted in Table C, generally there was some smoothening of the as-finished ball surface roughness in the dry running tests.

TABLE C

Surface Roughness Measurements on
Group 1 Orbital Balls (μm AA)

Test 1-1			Test 1-2		
1	2	3	1	2	3
0.055	0.024	0.098	0.035	0.025	0.025
0.029	0.057	0.065	0.053	0.026	0.029
0.031	0.048	0.075	0.022	0.026	0.025
0.020	0.026	0.063	0.020	0.052	0.033
0.049	0.045	0.063	0.040	0.026	0.029
0.033	0.039	0.044	0.026	0.035	0.023
Average			Average		
0.036	0.040	0.068	0.033	0.033	0.027

III. WEAR TESTING

A. Introduction

A considerable body of data is available on the behavior of silicon nitride ceramics (Si_3N_4) in the rolling contact bearing environment. Hot-pressed silicon nitride bearing components, either machined from billet stock or pressed to near net shape (NNS), have been shown to possess outstanding fatigue lives compared to the best available bearing steels in a ball testing configuration.[2,5] This superior life depends critically on the maintenance of basic material quality and surface integrity produced by both blank manufacturing and surface finishing processes. High density silicon nitride materials are also capable of operating at higher temperatures than possible with bearing steels and are essentially inert with respect to environmental corrosion. The objective of the wear testing portion of this program was to study the behavior of silicon nitride materials in a high temperature (540°C) rolling contact environment with an emphasis on developing engineering data for "dry" Si_3N_4/Si_3N_4 contacts with and without lubricant films.

A potential application of silicon nitride bearing components that utilizes its mechanical properties is as mainshaft bearings for limited life, high speed aircraft turbomachinery where both angular contact ball and cylindrical roller bearings are subject to corrosive environments and high temperatures. Roller bearings are typically used to support shaft dead weight and are subject only to maneuvering loads. The ball bearings support high magnitude thrust loads due to unbalanced aerodynamic forces reaching 2.1-2.4 GN/m^2 (300-350 KSI) maximum Hertz in low life, expendable engines. Lower stresses are present in longer life turbomachinery. Thus, the ball bearing environment constitutes a more severe application in which the silicon nitride material alleviates some environmental complications. Similar stress levels to metallic bearings are expected in properly designed silicon nitride bearings for this application.

Information is available on dry film lubrication of metals and some ceramics , mostly under conditions of sliding rather than rolling wear.[6,12] Successful dry-film lubrication performance depends on both the development of an integral bond between the film and the substrate as well as the development of a smooth, low friction surface on which relative surface motions induce minimal wear. Two of the most successful solid lubricants used in a wide variety of applications are molybdenum disulfide and graphite. Recent advances in sputtering these two materials have greatly improved these films bonding to a bearing component substrate. A more complex dry film lubricant used successfully at higher temperatures is VITROLUBE NPI 1220, a low-melting point glass bonded mixture of molybdenum disulfide, graphite, and

components which enhance both oxidation resistance and lubricity of the film. A final test series was reserved to evaluate some of the experimental surfaces discussed in Section IV of this resport. Due to the current unsuitability of these surfaces on which efforts to induce a more favorable surface stress distribution were made, molybdenum disulfide coated cages were substituted and evaluated in conjunction with coated balls as a fifth screening series.

B. Test Procedure

In order to study the potential of the ceramic/dry lube systems under conditions closely simulating the aircraft turbine environment, the rolling four ball tester, shown in Figure 8 was used. The contact stress levels, 2.8 GN/m^2 (400 KSI), used for this progam afford a degree of test acceleration with minimal danger of changing the wear mode to be expected in an aircraft turbine. Testing was done at 10,000 rpm spindle speed. A layout of the test program appears in Table D. The fifty hour test duration was felt to be sufficient, under the test conditions, to resolve differences in the various systems' rolling contact behavior. The carbon graphite cage used as an element separator was felt to provide self-lubricating cage contacts, as well as a potential source for a transfer film to lubricate ball-ball and ball-cup contacts. Both the carbon graphite cage and AISI M-1 tool steel cups were constant factors in all tests.

The silicon nitride materials discussed in Section II, were tested in the form of 12.7 mm balls. The selected lubricants were applied to the three support balls from which it was intended to be transferred during running directly to the track surfaces of the cup and the spindle ball. The support balls, cage and spindle ball were weighed before and after each test to determine the amount of wear occurring on each of the surfaces. Additionally, microscopic and SEM examinations were made to characterize the wear.

An ambient screening test series was conducted to select two lubrication systems for study at elevated temperatures. Modification of the four-ball test rig to allow operation up to 540°C are illustrated in Figure 9. In the four-ball tester, the test specimen, i.e. the spindle ball, is loaded through a vertical arbor against three orbital or support balls which orbit the spindle ball in a stationary cup race. The spindle ball is fixed in position with respect to the rotating arbor by a spacer rod slotted on the bottom to fit a flat sided projection ground on the top of the spindle ball. In addition to transmitting the desired load and drive torque to the spindle ball, the zirconia spacer rod performs as a thermal insulator during elevated temperature testing.

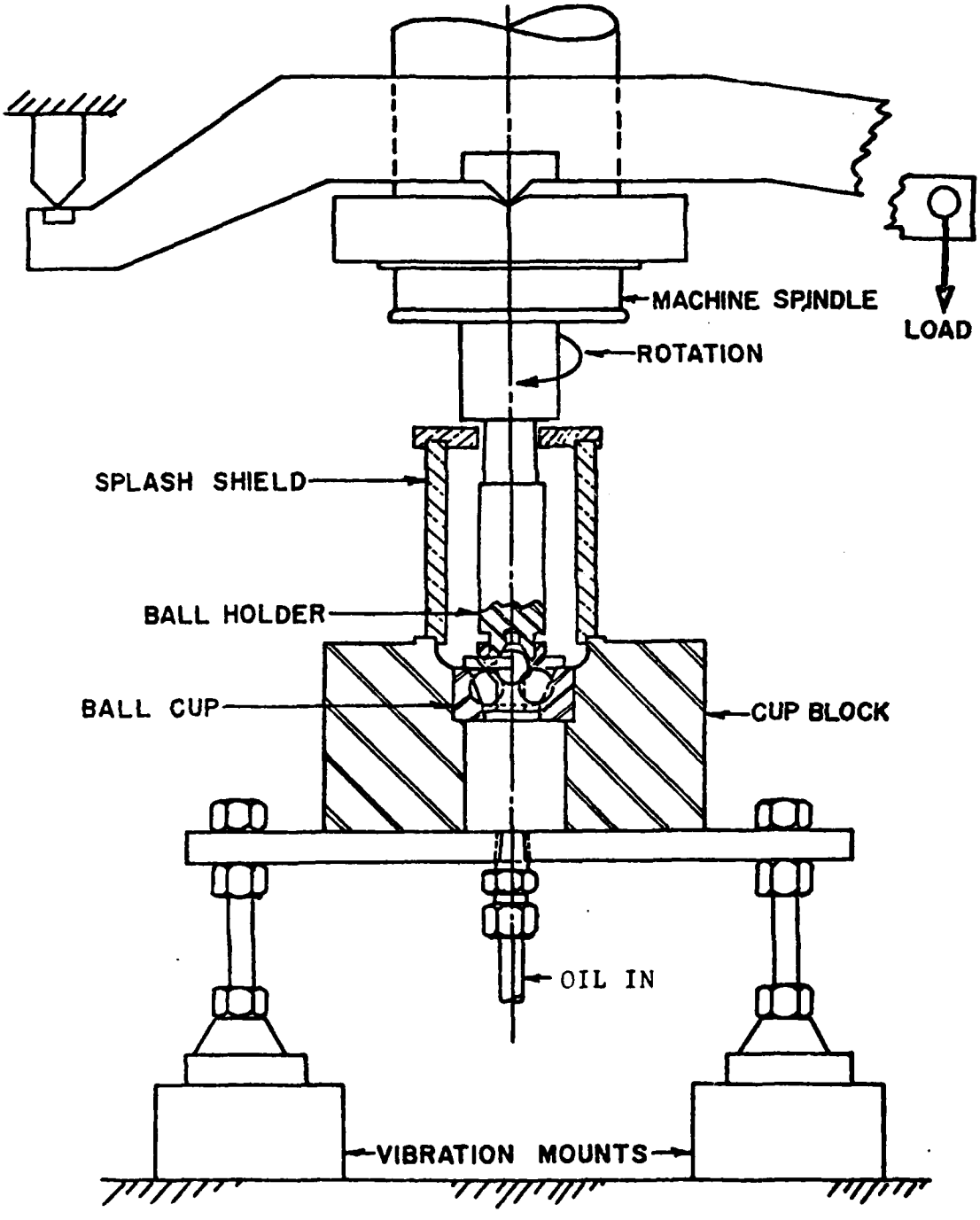

FIGURE 8 - Schematic drawing of ambient temperature rolling four-ball tester.

TABLE D

Rolling Four Ball Test Program
Si_3N_4/Si_3N_4 Contacts

Constant Conditions

10,000 rpm spindle speed

2.76 GN/m^2 (400,000 psi) contact stress

Graphite separator cage - Pure Carbon P-3310

M-1 steel cup

50 hour or vibration sensor test termination

Termination test duration

Variables

Contacts

a. Si_3N_4/Si_3N_4 - Baseline

b. Si_3N_4/molybdenum disulfide/Si_3N_4

c. Si_3N_4/graphite/Si_3N_4

d. Si_3N_4/vitrolube/Si_3N_4

e. Si_3N_4/molybdenum disulfide/Si_3N_4 plus molybdenum disulfide on graphite cage

Temperature

a. Screen above at ambient

b. Run two candidates @ 540°C

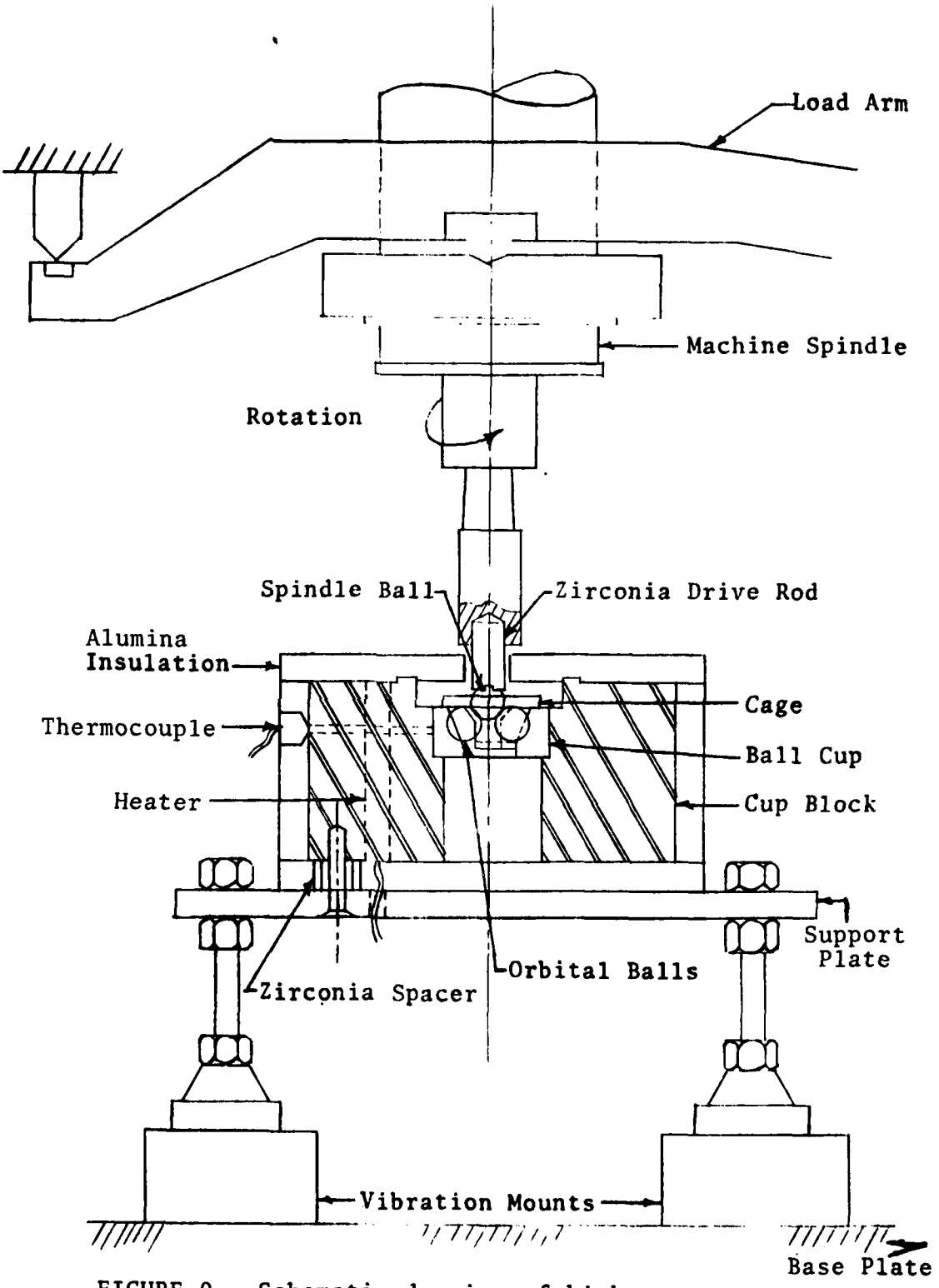

FIGURE 9 - Schematic drawing of high-temperature rolling four-ball tester.

The support balls are positioned in the cup race 120° apart and held in this relative position by a carbon-graphite (P-3310) cage manufactured by the Pure Carbon Co., Inc. The positioning of the support balls insures identical Hertzian stress at the three contact points between the spindle ball and the support balls. The contact angle of the assembly is controlled by the race design in the cup and the support and test ball sizes. The load, which determines the Hertzian stress at the contact points between the balls, is applied through the spindle by a dead weight and lever arm system. The spindle is driven by a constant speed AC motor through a pulley and belt drive system. The spindle speed can be varied by changing the ratio of the drive to driven pulley diameters. All testing in this program was performed at 10,000 rpm with a load calculated to produce a Hertzian stress at the ball-to-ball contact points of 400,000 psi.

The stationary cup is mounted in a cup block or housing which in turn is rigidly mounted to a support plate. Zirconia tube spacers located between the housing and support plate minimize heat transfer from the housing. The support plate is attached to the base plate of the tester through four vibration isolation mounts. To minimize further the heat input requirement and obtain a uniform temperature of the balls, cup and cup housing during elevated temperature testing, the cup housing is covered with a 1 inch thick layer of alumina fiber cloth. A photograph of the insulated cup housing, drive spindle and zirconia rod, support plate, vibration isolation, and base plate is presented in Figure 10.

To provide the elevated temperature, nine electrical resistance cartridge heaters (120V, 250W) are mounted in the cup housing. A shielded thermocouple senses the cup temperature and provides the on-off control signal to a Chromalox C76 solid state temperature controller. Any temperature from 40 to 540°C can be easily set and maintained within ±7°C by a single dial on the controller. An initial check-out test of the high-temperature rig was successfully performed with the temperature increased in incremental steps to 540°C.

Five series of rolling four-ball screening studies were conducted at ambient temperatures (∿30°C). For these tests, wear coefficients were calculated from the weight loss on the spindle ball. A bulk density of 3.22 g/cc was used for conversion to wear volume. The wear coefficient was then calculated using Archard's law;[12]

$$V = k\frac{Lx}{p}$$

where V = wear volume
L = load
x = sliding distance
p = hardness
k = wear coefficient

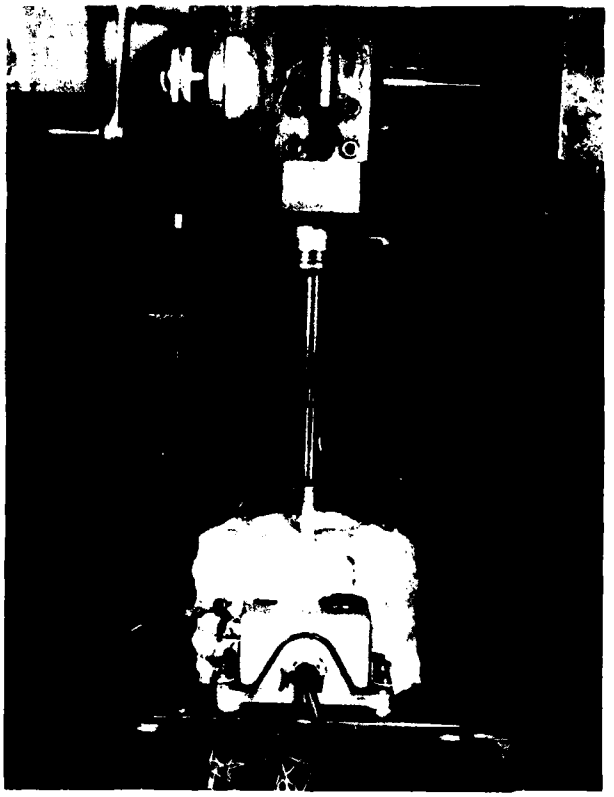

FIGURE 10 - Photograph of high-temperature test rig showing insulated cup block.

In the present case; the Hertz contact region is circular, the load distribution is parabolic, and the sliding distance per revolution of the spindle ball increases with distance from the center of the contact. The product of load and sliding distance was therefore expressed as a function of measured and calculated test parameters and integrated over the radius of the contact. The following equation for the wear coefficient has been established;

$$k = 0.129 \frac{P \cdot V}{S \cdot C \cdot (a^3) \cdot \sigma \max}$$

where k = wear coefficient

p = hardness measured at 1 kg load to be 1500 kg/mm^2 (14.71 GPa)

σ max = max. Hertz stress calcualted to be 2.76 GPa (400 ksi)

s = spin-to-roll ratio calculated to be 0.56 for the rolling 4-ball test with 40° contact angle

c = measured number of stress cycles on the spindle ball = 2.25 x number of revolutions for the 4-ball set-up

a = calculated contact radius of 0.083 mm (3.27 x 10^{-3} in)

Introducing the known constants in the above equation gives:

$$k = 2.149 \times 10^3 \frac{V}{c}$$

The calculated wear coefficients were used to compare the various dry lubrication systems studied in conjunction with SEM and optical microscopic examinations, as well as surface profilometry. Two series of high temperature at both 315 and 540°C were conducted with the "pure" silicon nitride contacts and the fifth ambient series, sputtered molybdenum disulfide on balls and cages, to document the high temperature wear properties.

C. Results

1. Ambient Temperature - The wear coefficients generated in the ambient temperature testing are presented in Table E. The wear tracks usually appeared glazed with very little visible surface damage such as chipping. As can be seen in the tabular summary, there is apparently very little, or no, beneficial wear effect from the dry film lubricants.

In some tests, both coated and uncoated, the wear rates were very low, resulting in less than ten microns (a few tenths of a thousandths of an inch) material removal from the bearing wear tracks, which may be acceptable, certainly in limited life missile and drone engine applications. In other tests, however, both coated and uncoated, the wear rates were five to ten times higher, which is probably not acceptable. These higher wear rates probably resulted from occasional lower density regions in wear tracks on these test balls made from NNS NC-132 blanks.

The shapes of the wear grooves on the spindle balls were traced using a rotary Talysurf (Figures in Appendix B). The amount of wear indicated by these traces generally correlated well with the weight loss measurements.

Calculations of the solid lubricant coating weight correspond roughly with the coated orbital ball weight losses given in Table E, so apparently most of the coating material was used up in these tests. There is also the distinct possibility that some graphite transfer film coating may form on the balls in these tests from the cage.

It can be seen from Table E that the computed dimensionless wear coefficient for the spindle ball is within the range of 10^{-6} to 10^{-5}. These values of wear coefficient are the same magnitude as those for oil lubricated steel measured previously at SKF by radiotracer techniques in NAVAIR studies of partial elastohydrodynamic (EHD) lubrication.[14] Apparently, dry rolling-spinning contacts of silicon nitride balls with a graphite cage have specific wear rates comparable to those of 52100 steel balls in the rolling four-ball tester at the ball surface asperity contacts that penetrate the very thin EHD film of MIL-L-23699, mineral oil and polyphenyl ether lubricants. As a further comparison of typical wear coefficients from the literature,[13] mild steel (RB 90 hardness) is reported to have a dry wear coefficient of about 7×10^{-3} and tungsten carbide about 10^{-6}, the low end of the range measured now for silicon nitride.

Typical scanning electron microscopy (SEM) photographs of the spindle ball wear tracks are given in Figures 11, 12 and 13. The uncoated ball test tracks with low wear are very smooth as shown in Figures 11a and b, whereas the uncoated test tracks with higher wear have an exfoliated appearance, shown in 11c and d. The exfoliated film is extremely thin and semi-transparent to electron-beam. In the low melting point glass bonded molybdenum disulfide solid lubricant (Vitrolube) coated orbital ball tests, the low wear spindle ball tracks were generally rather smooth, as shown in Figures 12a and c, but the high wear spindle ball in Figure 12d was somewhat rougher. Some portions of one low wear spindle ball track run against Vitrolube coated orbital balls had what appeared to be a surface coating (Figure 12b). The molybdenum disulfide sputter coated orbital ball tests also sometimes had a fragmented spindle ball surface layer shown in Figures 13c and d.

TABLE E

AMBIENT TEMPERATURE WEAR DATA

Group No.	Coating on Orbital Balls	Wt. Loss of Spindle Ball (10^{-3} g)	Wear Volume (mm^3)	Stress Cycles (10^6)	Wear Coeff. (10^{-6})	Wt. Loss of Orbital Balls (10^{-3} g)
1-1	None	0.33	0.102	70.20	3.1	0.25
1-2		0.45	0.139	71.82	4.2	0.34
1-3		2.36	0.731	69.53	22.6	3.19
1-4		0.15	0.046	66.15	1.5	0.15
2-1	Vitrolube	0.49	0.151	67.30	4.8	98.0
2-2	NPI1220	2.73	0.845	69.03	26.3	106.0
2-3		0.67	0.207	68.04	6.5	100.5
3-1	Sputter Coated	1.83	0.567	67.50	18.1	15.2
3-2	MoS_2	1.67	0.517	64.80	17.1	14.5
3-3		0.40	0.124	67.50	3.9	13.7
4-1	Sputter Coated	2.00	0.619	70.61	19.0	4.05
4-2	Graphite	1.70	0.526	67.50	16.7	3.92
5-1	Sputter Coated	0.35	0.108	30.10	7.7	2.37
5-2	MoS_2*	1.73	0.536	62.10	18.5	3.55

*The cage and cup were also sputter coated with MoS_2 in these tests.

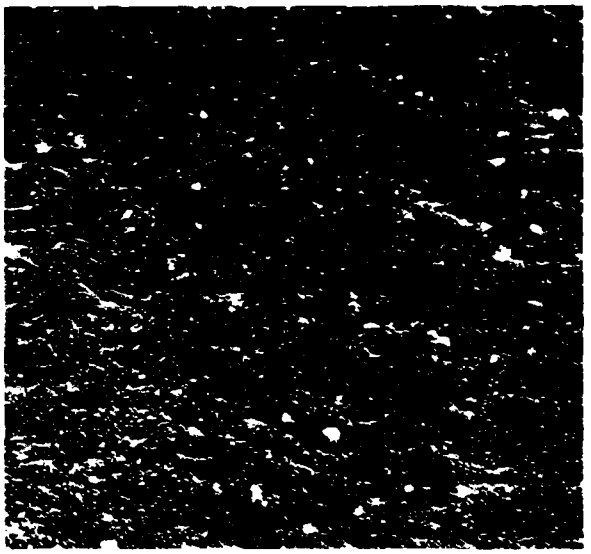

2500X

a. Low wear spindle ball from Test 1-1

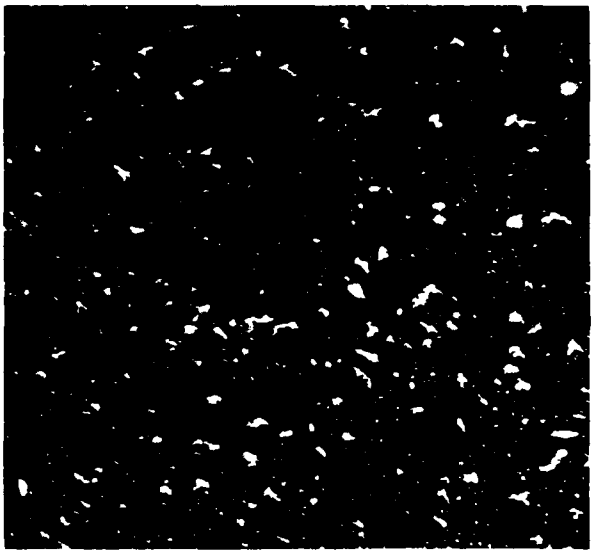

2500X

b. Low wear spindle ball from Test 1-2

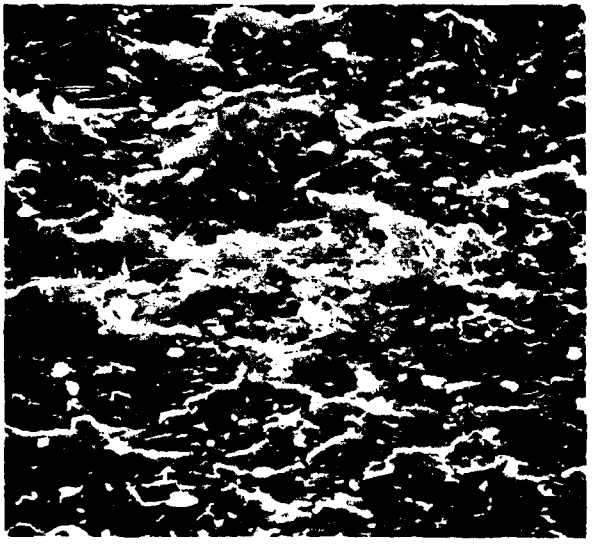

2500X

c. Center of track on high wear spindle ball from Test 1-3

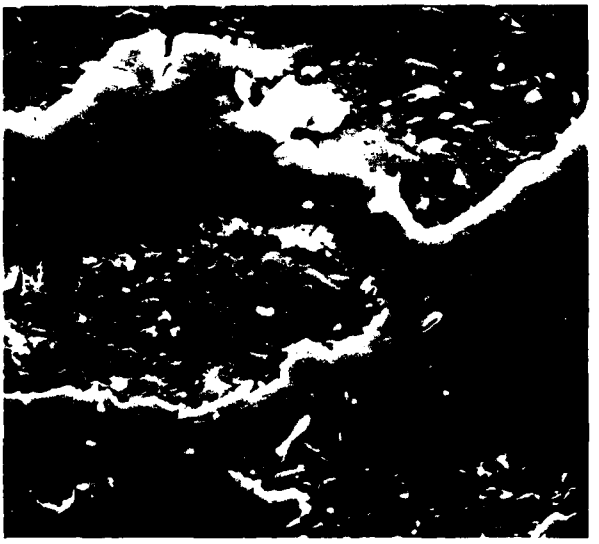

2500X

d. Near edge of track on high wear spindle ball from Test 1-3

FIGURE 11 - Comparison of wear tracks on uncoated NC-132 balls tested with graphite cage. Secondary Emission SEM

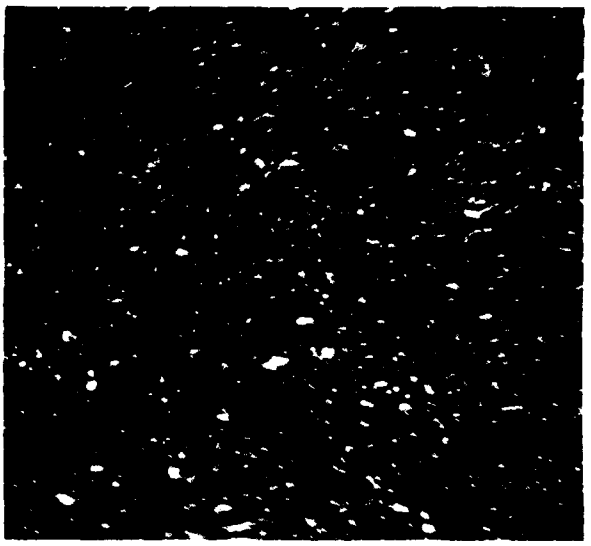

2500X

a. Smooth part of track from low wear Test 2-1

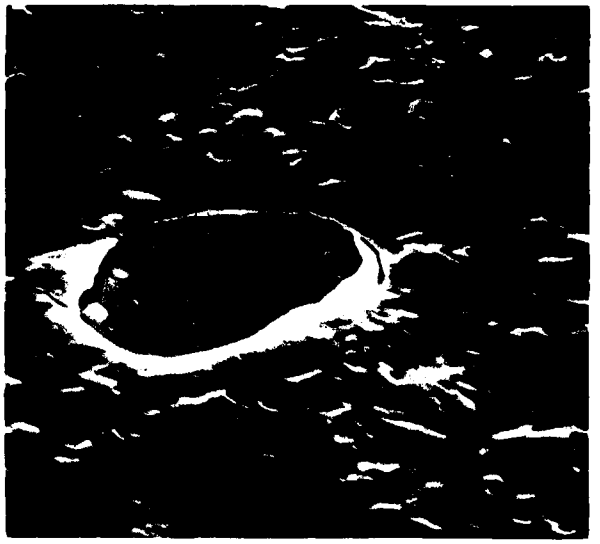

2500X

b. Rough part of ball track from low wear Test 2-1

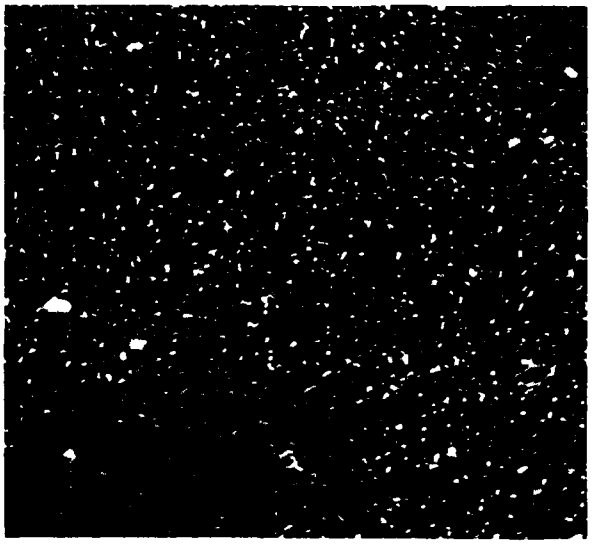

2500X

c. Center of ball track from low wear Test 2-3

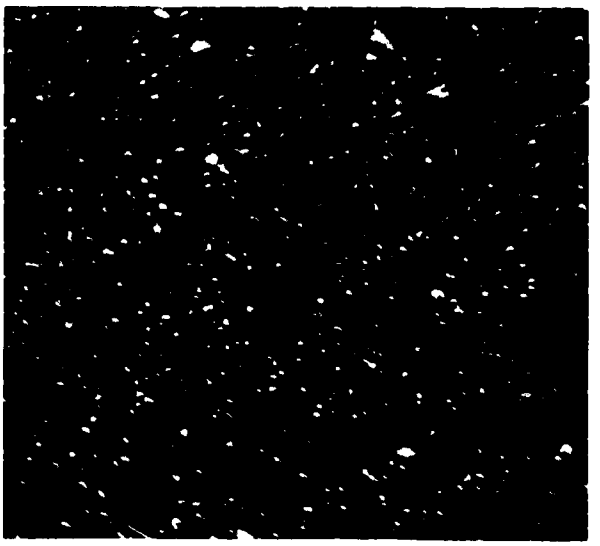

2500X

d. Center of ball track from high wear Test 2-2

FIGURE 12 - Comparison of wear tracks on NC-132 spindle balls tested with Vitrolube coated orbital balls and graphite cage. Secondary Emmission SEM

500X

a. Center of ball track from Test 3-1

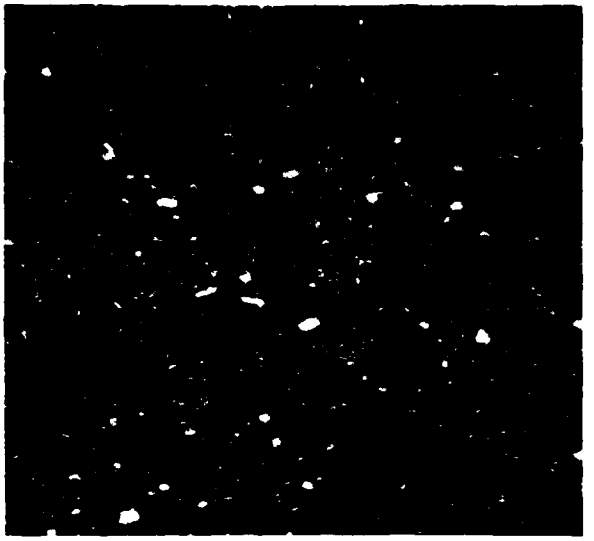

2500X

b. High magnification of Figure 3a

500X

c. Center of ball track from Test 3-2

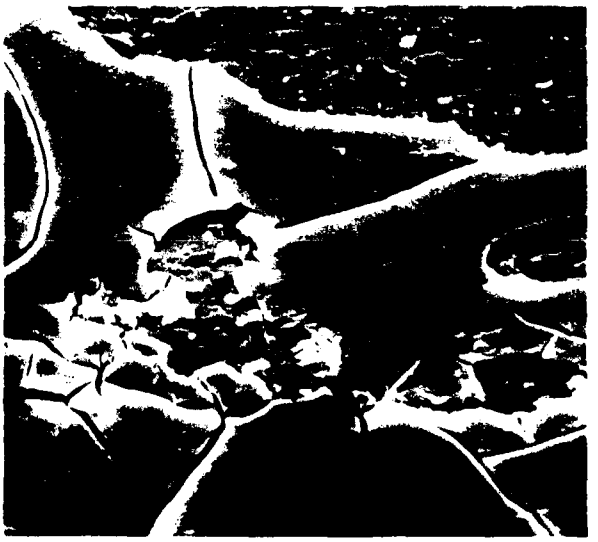

2500X

d. High magnification of Figure 3c

FIGURE 13 - Comparison of wear tracks on NC-132 spindle balls tested with MoS_2 sputter coated orbital balls and graphite cage

Silicon and carbon x-ray scans with a wavelength dispersive microprobe on the spindle ball track from the high wear uncoated Test 1-3 showed evenly distributed silicon and only very slight but evenly distributed carbon, so that the exfoliated surface on this track may be wear damage to the silicon nitride itself. The reason for this single high wear test is not clear. Figure 14 shows the molybdenum disulfide coated orbital balls (2-1). The surface layer in the SEM view in Figure 14a apparently is not composed of as much silicon nitride as the surface under this layer, although it does not contain large quantities of molybdenum either. Molybdenum was found in detectible quantities in the surface depressions on the orbital balls from this same test, although these orbital ball surfaces did not exhibit the surface layered appearance found on the spindle ball shown in Figure 14a.

Figure 15 shows the surface layer on the spindle ball run against molybdenum disulfide sputter coated orbital balls (3-2), demonstrating that this layer contains molybdenum. This layer appears friable and apparently is not very protective to the surface since the wear rate was high in this test. The repeat test with this coating giving a lower wear rate (3-3) did not have this layer in the spindle ball wear track and the x-ray scan showed very evenly distributed silicon with very little but even molybdenum concentration.

Since molybdenum disulfide is detrimentally affected in its lubricating ability by water vapor, some effort was made in the last group of sputter coated tests (5-1 and 5-2) to desorb all water vapor from these coatings and keep them dry by operating at slightly elevated temperature. Also, the cages and cups were sputter coated, for these tests, to help provide an increased lubricant film supply to the spindle ball and to protect the relatively higher surface energy steel cup tracks.

In these "ambient" temperature tests (5-1 and 5-2) all new parts were used. The components were heated to 80°C (180°F) and maintained at that temperature for two hours before starting the test. Temperatures were then maintained at this level throughout the test runs. A test ball wear loss of 349 micrograms occurred after 22.7 hours of operation in Test 5-1 and 1733 micrograms after 46 hours of operation in Test 5-2. These results show no improvement over the prior tests run at room temperature with no lubricant and with MoS_2 on the support balls only.

2. High Temperature Testing - Two groups of elevated temperature rolling four-ball tests were conducted dry, and the test data and analysis are summarized in Table F. The first hot test (1-5) was run using uncoated balls with a P-3310 graphite cage and M-1 tool steel cup. Previous testing at ambient temperatures did not indicate any significant improvement in wear performance using solid lubricant coatings compared to

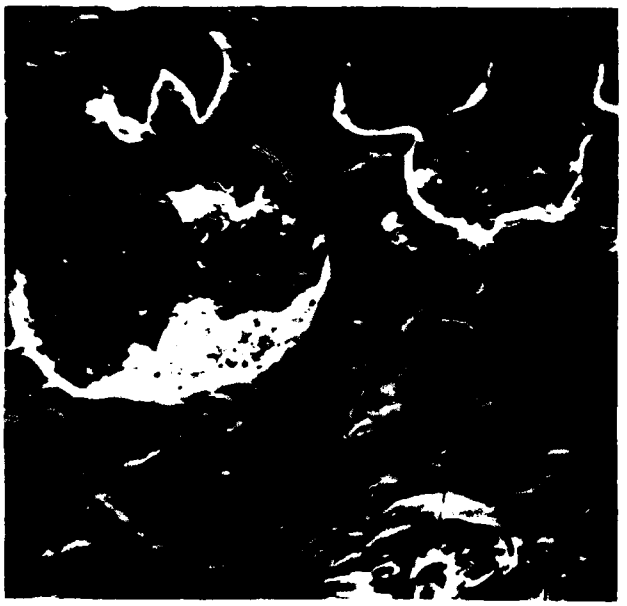

2500X

a. SEM photo of surface in rough part of ball wear track

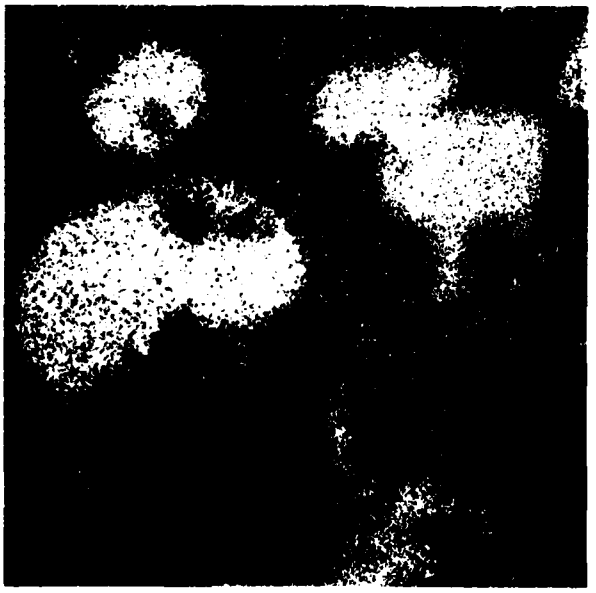

2500X

b. Silicon concentration map of view in a

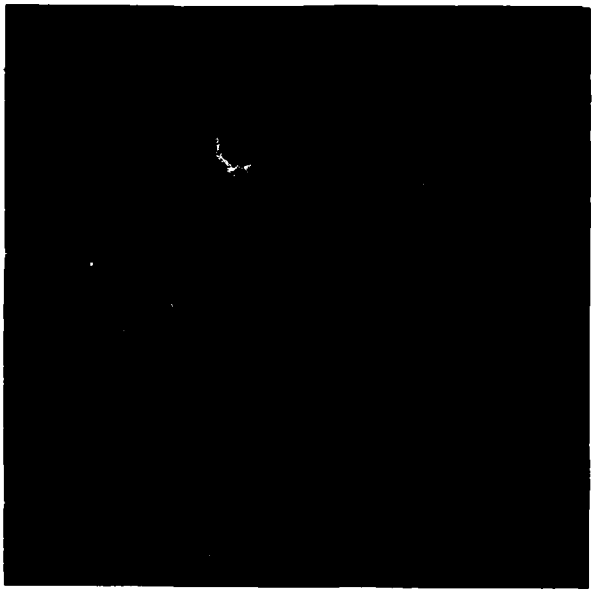

2500X

c. Molybdenum concentration map of view in a

FIGURE 14 - Microprobe analysis of surface layer on NC-132 spindle ball track after Test 2-1 with Vitrolube coated orbital balls and graphite cage.

2500X

a. SEM photo of surface in center of ball wear track (SE)

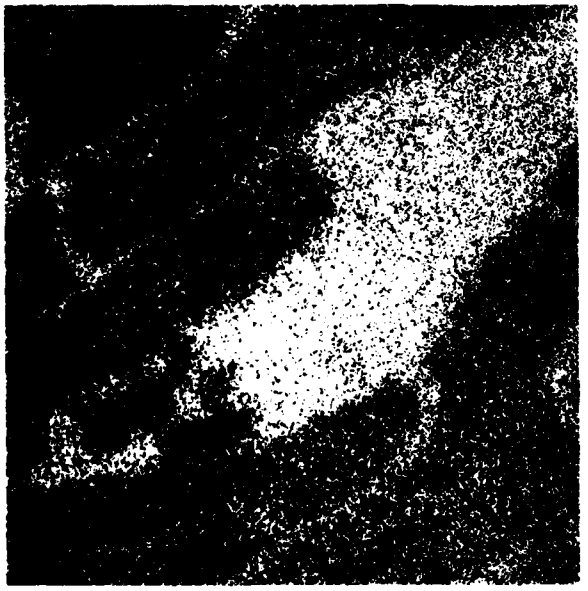

b. Silicon concentration map of view in a

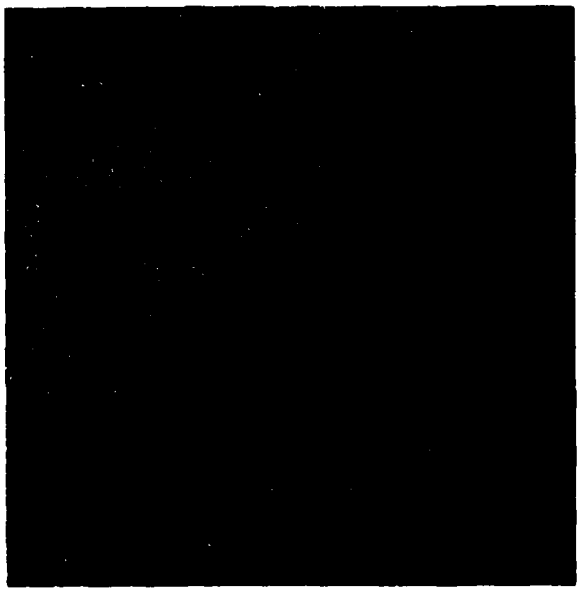

c. Molybdenum concentration map of view in a

FIGURE 15 - SEM & microprobe analysis of surface layer on NC-132 spindle ball track after Test 3-2 with MoS_2 sputter coated orbital balls and graphite cage.

TABLE F

HIGH TEMPERATURE WEAR DATA

Group No.	Test Temp. (°F)	Coating On Orbital Balls	Weight Loss of Spindle Ball (10^{-3} g)	Wear Volume (mm^3)	Stress Cycles (10^6)	Wear Coeff. (10^{-6})	Weight Loss of Orbital Balls (10^{-3} g)	Cage Weight Loss (10^{-3})
1-5	600	None	0.21	0.066	33.08	4.3	2.04	--
1-6	1000		4.63	1.426	15.12	202.7	16.4	--
1-7	600		0.58	0.179	1.82	211.8	-0.01	5.18
1-8	600		0.43	0.132	34.02	8.3	1.63	57.7
1-9	800		0.77	0.236	13.37	37.9	0.66	42.2
5-3	600	Sputter Coated MoS_2*	0.58	0.178	31.05	12.3	2.40	31.8
5-4	800		--	--	3.78	--	--	

*The cage and cup were also sputter coated with MoS_2 in these tests.

initially uncoated balls with the graphite cage, which may provide some beneficial solid lubricant transfer films on the balls during operation.

The first test was initiated after the temperature of the housing, cup, and balls were increased to 315°C (600°F). After 25 hours of operation at 315°C, the test was terminated to check the wear rate. The loss in weight of the spindle (test) ball was 214 micrograms. The total loss in weight of the three orbital balls was 2035 micrograms. Thus, the wear rate of the test ball was quite low and very similar to that obtained previously in the ambient temperature tests. However, the wear rate of the orbital balls was approximately ten times greater than would be expected when compared to previous tests. In all four ambient temperature tests run with uncoated balls, the total loss of material from the orbital balls was approximately the same as the loss on the test ball. The possibility of an interaction with the M-1 steel cup cannot be discounted.

The same test elements used at 315°C were then reassembled for the second hot test (1-6). The test was initiated when the temperature of all parts had reached 370°C (700°F), after which the test temperature was increased to 540°C (1000°F) in approximately 2 hours. After 11.2 hours total running time, the test was terminated by excessive vibration causing automatic vibraswitch shutdown of the test machine. Inspection of the test spindle ball and orbital balls following the 540°C test showed that 4633 micrograms had worn off the test ball and a total of 16407 micrograms from the orbital balls. Optical inspection of the balls showed that a thin layer of material had exfoliated from varying percentages of the surface of the orbital balls and wear track of the test ball. Approximately 70 percent of the surface of one orbital ball had exfoliated, 10 percent of another, and 1 percent of the third.

The wear in the cage pockets was excessive with the pattern indicating that two orbital balls were driving the cage and the third ball was being driven by the cage at the end of the test. This condition could have resulted from the change in orbital ball speed produced by the difference in diameters due to varying degrees of wear. The excessive wear probably resulted from a degradation of the graphite cage material at 540°C which showed some evidence of oxidation as well as the roughened condition of the test components from the earlier 315°C test.

The wear coefficient of 2×10^{-4} measured on silicon nitride in the first test at 540°C is very high, of course. Assuming that a graphitic transfer film was present during the lower temperature tests; the very thin, high surface area nature of such a film would almost preclude its existence at higher temperatures in the presence of oxygen.

A third elevated temperature test (1-7) was run at 315°C with "pure" silicon nitride contacts to verify the results of the first test at this temperature. New balls and a new cage were run in this test; other variables were identical to the previous 315°C study. After 1.35 hours of operation the test was terminated by a vibraswitch shutoff. A check of the spindle ball showed that a rough wear track had produced the shutoff. The material worn from the spindle ball was 583 micrograms. Examination of the support ball showed surface damage and a weight gain. SEM and microprobe micrographs of the orbital balls are presented in Figure 16. The ball surface in Figure 16a is very similar to the as-finished surfaces of these NC-132 balls, except for what appear to be deposits. Microprobe scans in Figures 16b and c indicate that these deposits contain iron covering the silicon nitride; probably transferred steel wear debris from the M-1 steel cup. The bright regions in these maps indicate presence of the element analyzed for, whereas the dark regions indicate its absence. The carbon map in Figure 16d shows some carbon, but very little above background, and only slight concentrations in surface depressions expected for soft graphite wear debris from the cage pockets against which this ball surface had rubbed during the test.

A new M-1 steel cup was used in the next test (1-8) at 315°C as another attempt to corroborate the good results of the first test; run previous (1-5). This test ran uneventfully for the full 25 hours, after which the spindle test ball was shown to have lost only 429 micrograms from wear. The orbital balls lost 1634 micrograms, which is less than the 2035 micrograms wear loss on the orbital balls in the previous 315°C test (1-5), but still more than the typical orbital ball wear loss in previous ambient temperature tests. This higher loss may be characteristic behavior for this test system at elevated temperatures.

The same test parts used in the above 315°C test (1-8) were run again at 430°C in the next test (1-9) in a manner similar to that used for the previous 540°C test (1-6). This temperature was chosen to reduce the amount of transfer film oxidation occurring at the higher temperature. This test was terminated after 9.9 hours by a vibraswitch shutoff. The spindle ball wore 766 micrograms and the orbital balls 662 micrograms, which is consistent with the ambient temperature test pattern but at somewhat higher wear rate than at lower temperatures but not as high as at 540°C (1-6) or in the second 315°C test (1-7).

Figure 17 shows very distinctly the graphite deposits on the spindle ball track from the heavy cage pocket wear in the 540°C uncoated ball test (1-6). This graphite obviously is not adherent enough to prevent silicon nitride wear. The pattern on the silicon map in Figure 17c indicates that other species are present on the worn silicon nitride surface, which was not explored further in this analysis. Even though there was heavy

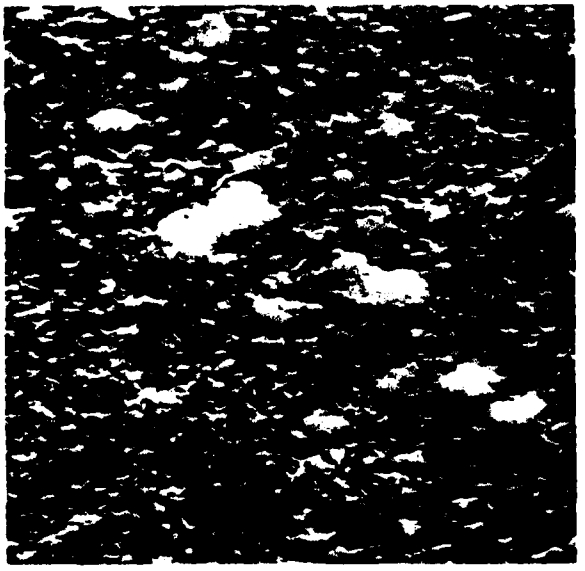

1000X

a. SEM photo of typical surface

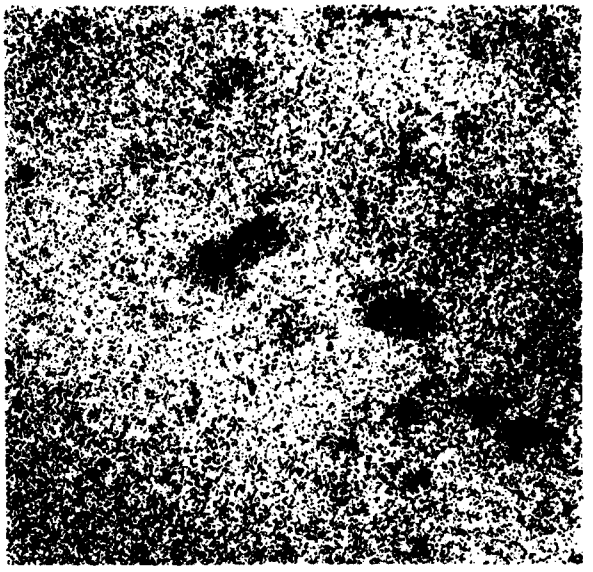

1000X

b. Silicon concentration map of view in a

1000X

c. Iron concentration map of view in a

1000X

d. Carbon concentration map of view in a

FIGURE 16 - Microprobe analysis of surface on NC-132 orbital ball after Test 1-7 at 315°C (600°F) with uncoated balls and graphite cage.

1.7X

a. Heavy wear in cage pocket

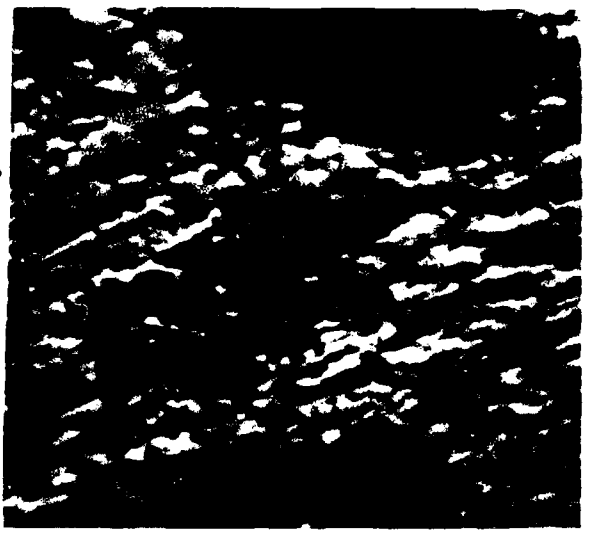

1000X

b. SEM photo of surface in center of ball wear track

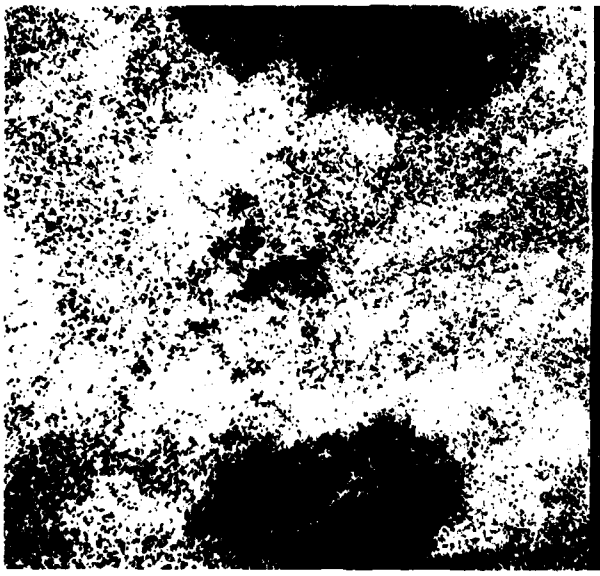

1000X

c. Silicon concentration map of view b.

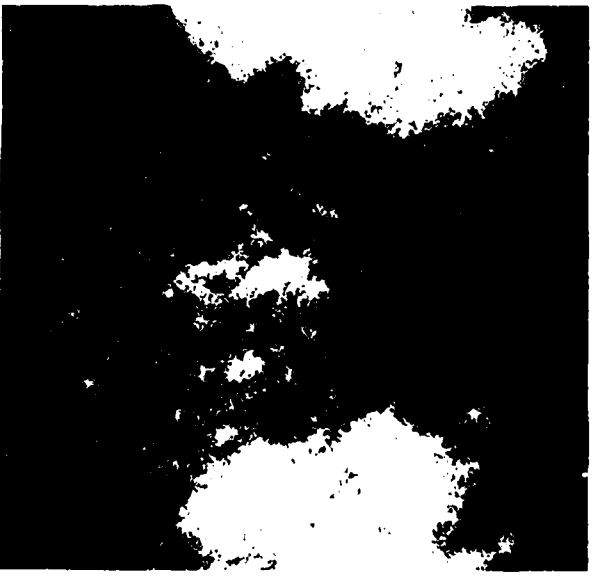

1000X

d. Carbon concentration map of view in b.

FIGURE 17 - Cage pocket wear and x-ray analysis of deposits on wear track of NC-132 spindle ball after Test 1-6 at 540°C (1000°F) with uncoated balls and graphite cage.

wear of both the cage and the balls in this 540°C test, the test elements maintained structural integrity.

Test 5-3 was performed at 320°C with the same components used in Test 5-2 except for the test ball which was new. After 23 hours of testing, a wear weight loss of 578 micrograms had occurred on the spindle ball. During the test, the cage turned to a light gray-blue color indicating that oxidation of the surface had probably occurred at the elevated temperature. An additional test (5-4) was attempted with all the same components used in Test 5-3, but at a temperature of 430°C. After only 2.8 hours of operation, the cage broke terminating the test. The weight loss of the test ball was not determined since appreciable exfoliation of the support balls had occurred which was considered to have made the results unreliable.

D. Conclusions

The wear data shown in Tables E and F show some scatter among replicate tests. Much of this scatter is believed to be caused by variations in the occurrence of low density regions in the wear tracks on these pressed to shape balls. The origin of some of this scatter at the high temperatures also is felt to be due to the nature of the graphitic transfer film present (or not present) during the tests. It is also clear that the condition of the M-1 steel cup used to support the orbital balls contributed to some of the high temperature variability; for future work at high temperature silicon nitride support may be necessary to eliminate this variability. Alternate cage materials may provide more durable, oxidation resistant transfer films. Any significant lubrication that did occur during these tests came from the graphite cage. There is no clear advantage to any of the dry film lubrication systems screened in ambient testing. The integrity of the NC-132 balls under conditions of high wear is significant.

The effect of temperature on wear rate was analyzed by making logarithmic probability plots of these wear data. Figure 18 is such a plot of all the ambient temperature data given in Table E. The center line in Figure 19 is a plot of the data in Table F, without counting Test 1-7, which apparently was unduly influenced by the steel cup wear, as shown by SEM and x-ray analysis. The mean wear coefficient of both these plots is 8×10^{-6}, indicating that the silicon nitride ball wear performance is not significantly different at 325°C than at ambient temperature. Although the wear data available at higher temperatues are quite limited (certainly too few to plot), there is some indication from Table F that the wear coefficient increases by about a factor of five for every 110°C higher temperature above 315°C. The influences of oxidation of the graphitic transfer film and the M-1 cup are not clear at this time.

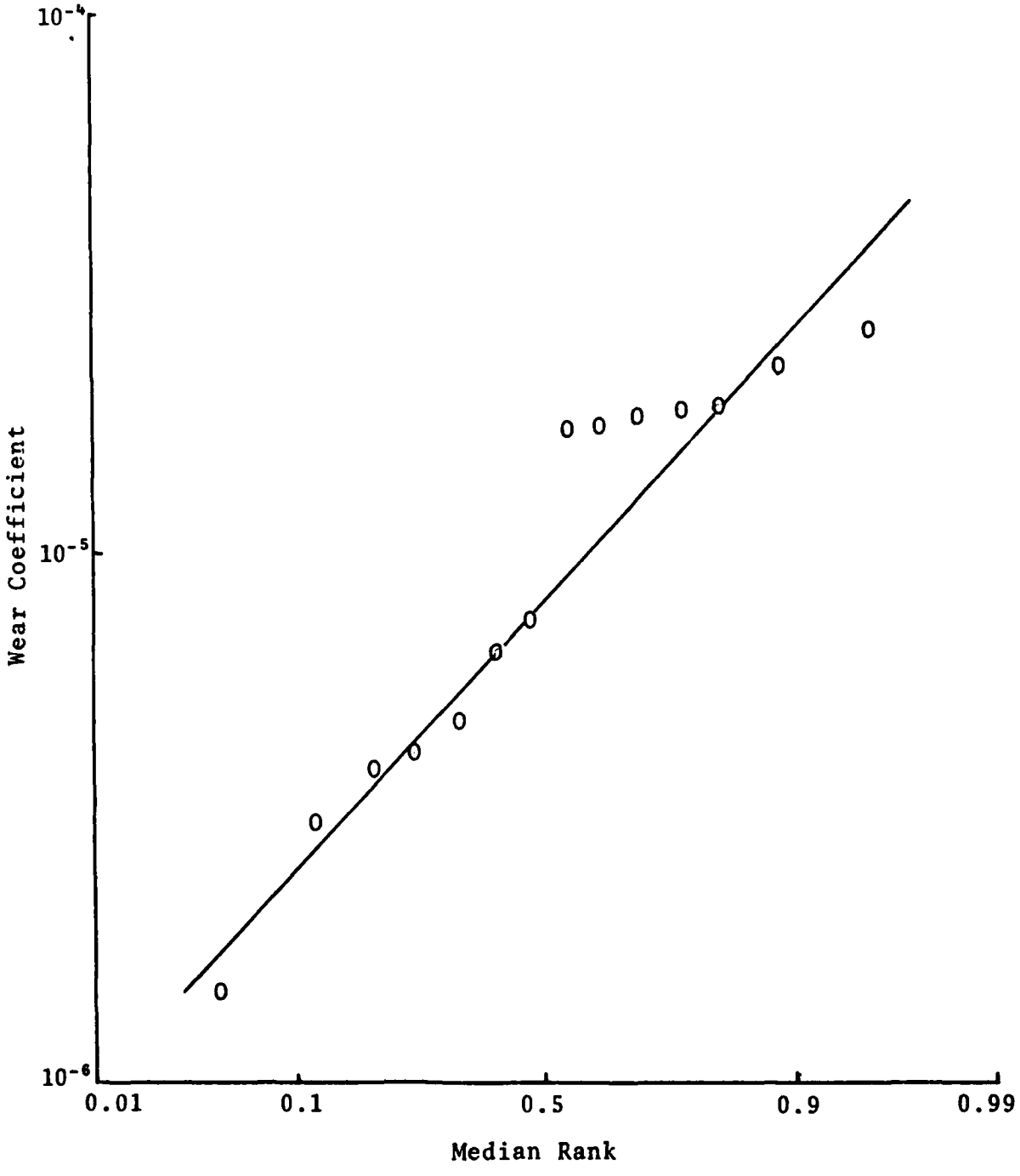

FIGURE 18 - Log-normal probability plot of ambient temperature wear coefficients (all data).

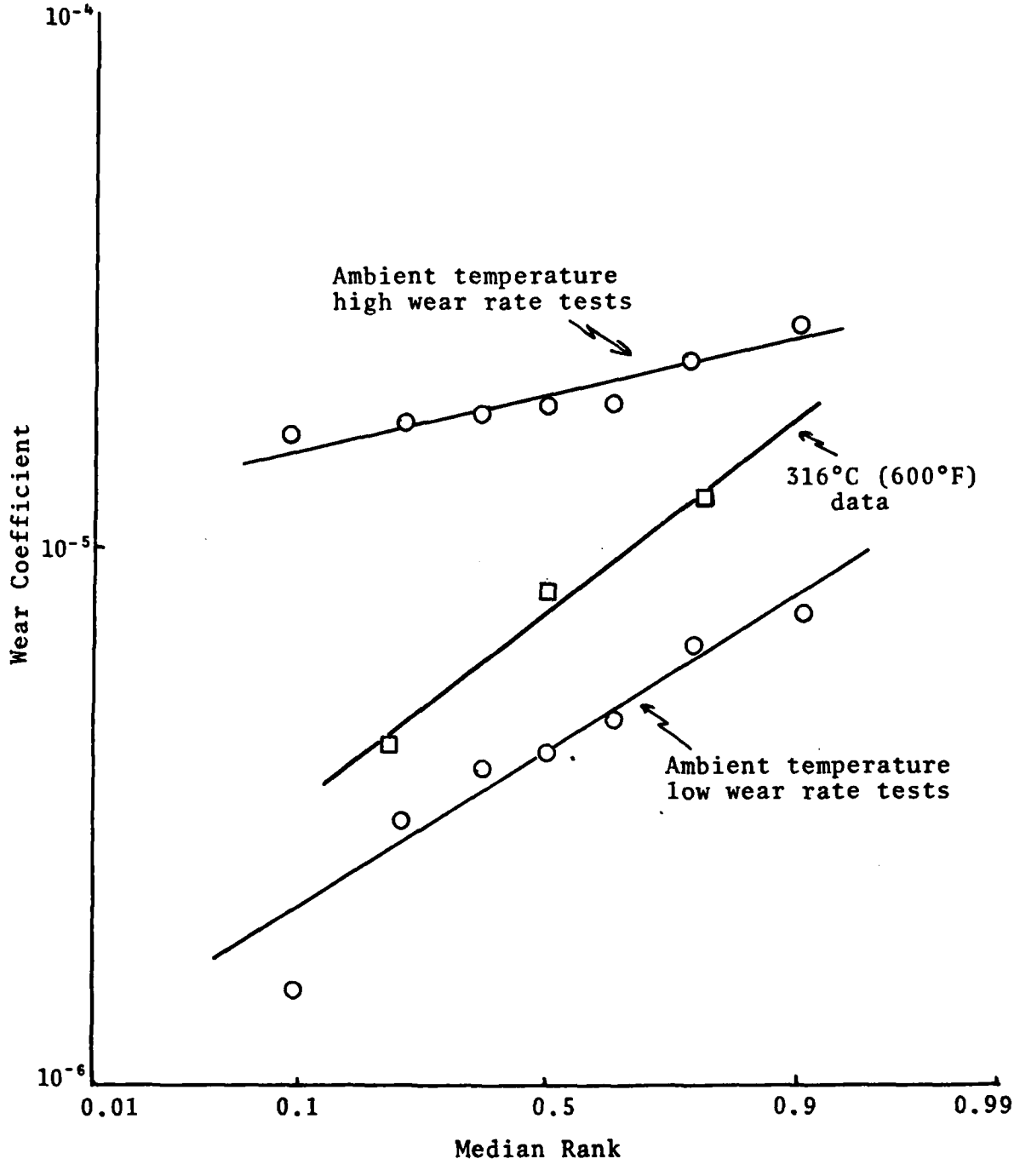

FIGURE 19 - Log-normal probability plot of wear coefficients at 315°C (600°F) and bimodal analysis of ambient data

The data points plotted in Figure 18 also seem to have a bimodal appearance, suggesting two distinct populations of wear inducing defects in the silicon nitride surface.[15] Therefore, these ambient temperature data were divided into two subgroups having low and high wear coefficients, respectively, and then were replotted in Figure 19. If the high wear subgroup could be eliminated, the data seem to indicate that a mean wear coefficient of 4×10^{-6} might be realized.

The practical significance of these wear coefficient values in dry operating bearing design can be appreciated by considering the following formula for bearing wear life taken from Archard:[13]

$$t = d \frac{p}{k} \frac{1}{PV}$$

where

t = bearing life from wear failure
d = maximum acceptable wear depth
p = DPN hardness of bearing material
k = wear coefficient
P = nominal load pressure
V = sliding velocity

Assuming an acceptable wear depth to failure in the tracks of a typical gas turbine engine bearing of 0.3 mm (0.012 in.) and a typical PC-value for such a bearing of 100 $GN/m^2 \times mm/sec$ performance [13], this formula predicts a wear life for a dry silicon nitride turbine bearing having 4×10^{-6} wear coefficient and 14.7 GPa (1500 kg/mm^2) DPN hardness of

$$t = 0.3 \frac{14.7}{4 \times 10^{-6}} \frac{1}{100} = 11{,}025 \text{ seconds; about 3 hours}$$

which is probably satisfactory for low-life expendable turbines, but not for longer life machines. Since no improvement in wear coefficient was shown in the tests reported here with the few solid lubricant films tested, yet such improvements have been demonstrated repeatedly before with copious solid lubricant supply systems [7-11], there is a great potential for realizing dry bearing wear lives many times longer than that computed above.

IV. EXPERIMENTAL MATERIALS TESTING

A. Introduction

The rolling contact bearing environment is typified by high magnitude Hertzian stress fields. The stress distribution is such that the magnitude of the tensile stress component decreases exponentially with the distance from the material surface. The reasonably expected failure mode for dense ceramics in the rolling contact environment is tensile given that brittle materials are more sensitive to crack propogation from "flaw-opening" loading modes than the reverse. Thus, alterations yielding a stronger surface layer (in tension) should improve the material's performance.

Such strengthening mechanisms are in wide use in both ceramic and metallic materials. Chemical or thermal tempering of glass is widely employed to increase a glass' resistance to tensile failure; strength may be increased by an order of magnitude. Case hardening is a similar mechanism utilized in the metals industry. Inducement of a residual compressive stress in the surface of a material increases the tensile force required to initiate failure. Several methods of inducing such a favorable stress distribution were attempted in this program. The resulting surfaces were evaluated by both flexural and static Hertzian indentation testing.

B. Chemical Stuffing

Replacing the silicon in silicon nitride with larger cations will crowd the silicon nitride matrix; resulting in a residual surface compressive stress. This technique is similar to chemical strengthening of glass. There are approximately 25-30 stable nitrides; of these about 15 are more thermodynamically stable than silicon nitride. See Table G. Periodic table groups 1a and 2a form stable nitrides but all react with water readily. Groups IIIB, IVB, and VB form the most stable nitrides. Of these only the substitution of Ti, Zr, Hf, Nb, or Ta for Si will result in a compressive surface stress. Chemical exchange of these ions should be possible. One solvent that dissolves all of these materials is Hf. Of the remaining elements only B and Al form nitrides more stable than silicon nitride. BN formation would not result in a compressive stress and AlN decomposes very slowly in boiling water.[16] Successful "stuffing" of a silicon nitride surface is only possible with a few species. Hafnium and niobium are of limited availability. Studies proceeded with titanium, zirconium and tantalum substitutions.

Preliminary studies indicated that some exchange of metallic ions in the silicon nitride materials occurs in room temperature concentrated hydrofluoric acid solutions. Solutions of Ti, Zr, and Ta metals in 0.1 m and 0.2 m concentrations were prepared

TABLE G

Refractory Nitrides-Thermodynamic Properties

Nitride	Enthalpy of Formation[17] Kcal/gr-atom of Nitrogen	Thermodynamic Driving Force, Kcal/gaN $\Delta H_{fo\ Si_3N_4} - \Delta H_{fo}$ species	Molar Volume Increase for Complete Exchange	Comments
Li_3N	-47	-3		Hydrolyzes
BeN_2	-68	-24		Hydrolyzes
Mg_3N_2	-55	-11	0.68	Hydrolyzes
Ca_3N_2	-53	-9	1.50	Hydrolyzes
Sr_3N_2	-47	-3		Hydrolyzes
ScN	-75	-31		
Yn	-71	-27		
LaN	-71	-27		
TiN	-80	-36	0.08	Sol. HF; aqua regia
ZrN	-87	-43	0.34	Sol. H_2SO_4 HF, aq. reg.
VN	-52	-8	-0.03*	Aq. reg.
HfN	-88	-44	>0.34	
TaN	-59	-15	0.08	Sol. HF, HNO_3 Aq. reg.
BN	-61	-17	0.0	Hot acids
AlN	-76	-32	0.14	
Si_3N_4	-44	0	0	HF, HNO_3

*Shrinkage

and silicon nitride test samples were immersed in them for two and three hour periods. For the 0.2 m solutions the Ti and Zr specimens showed small, but resolvable, density increases of 0.012 and 0.015 w/o, respectively after three hours exposure. The Ta specimens were unchanged. Surface XRD did not resolve any phase changes as the levels of exchange expected from weight changes were beyond x-ray diffraction's resolution.

A flexural strength study was carried out to determine if the desired surface characteristics had been obtained. The results are presented in Table H. It is clear that the treatments decreased the measured strength below that of untreated samples.

TABLE H

Flexural Strength Measurement-Chemically Stuffed Hot-Pressed Silicon Nitride

Sample	Mean (MN/m^2)	σ (MN/m^2)	n
Untreated	892	22.5	5
HF etch	712	67	5
Titanium ion	727	17	4
Zirconium ion	664	112	4
Tantalum ion	736	92.5	4

Fracture analysis showed a clear fracture origin for every sample that had been exposed to the HF acid medium. Normally, NC-132 silicon nitride tensile surfaces show several, or no, fracture origins in "non-machining" induced failures. It is felt that the use of 38 percent HF as an exchange medium is not suitable due to an excessive fluorine activity, causing more damage through etching mechanisms than the cationic stuffing was capable of repairing. This theory is supported by the high standard deviations in strength noted in most "stuffed" samples. Further analysis with lower fluorine potentials or, conversely, high cation potentials is clearly in order.

C. Surface Oxidation

Silicon nitride is thermodynamically unstable with respect to oxidation at all temperatures. Below 600°C the rate is vanishingly small in air. Partial solution of oxygen in the silicon nitride lattice will result in some surface "stuffing" for a compressive stress. Of equal concern is oxidation of a grosser scale in which sharp cracks (flaws) in the material are filled in; increasing the energy required to propagate a crack.

Such an oxidation film has been demonstrated to increase flexural strengths in NC-132 silicon nitride.[18] The development of the oxidation film is shown in Figures 20, 21, 22 and 23. Weight gains on all samples were less than 100 micrograms and unresolvable on the balance used. Figure 20 is a micrograph of the standard lapped surface. The depth of the pullouts from the lapping procedure is less than 0.5 μm. As both temperature and exposure time increase there is a progressive filling of the pullouts in the surface. Surface x-ray diffraction, as expected, did not resolve any phase shifts, attesting to the thinness of the reaction layer.

D. Hertzian Indentation Testing

The nature of the Hertzian stress field has been recently discussed in reference to ceramic materials.[19-21] It has also been shown that Hertzian failures of hot pressed silicon nitride materials detected by acoustic emission can be used to detect large changes in surface properties.[3] An instrument setup has been described and some results for ground NC-132 surfaces have been tabulated.[3]

The NC-132 lapped surfaces were indented with a 4.75 mm diameter tungsten carbide ball at a loading rate of 0.05 mm/minute. Failure was detected by acoustic emission monitors and both failure load and surface condition tabulated. The geometry of the failure zone was tabulated for each indentation by optical measurement in either darkfield illumination or crossed Nicols. Micrographs of typical failure surfaces are presented in Figures 24 through 28 and illustrate some features of the failure mechanism. Reflected light does reveal the crack in some samples, but its outline is indistinct, see Figure 24. Of more interest is the notable difference in contact zone inside the crack. The standard lapped surface shows very slight surface distress in the compression zone and only the geometric center of the indented area where compressive stresses are highest. The oxidized surface shows a greatly distressed contact zone. There has been local reorientation of surface grains in oxidized surfaces under even slight compression (at the zone edge) that reflects considerably more light than uncompressed material.

It is unlikely that this is plastic deformation and the conclusion must be reached that localized, on the scale of single grains, brittle failure has taken place in the compression contact zone of oxidized samples. Even though the sample still failed in tension, cyclic compressive stressing of oxidized surfaces would be expected to result in a roughening of the surface as particles of oxidized material break out. Similar behavior was noted at both 600°C and 750°C. Dark field illumination of the same fields bears out the same analysis; see Figure 25. Dark field illumination is particularly sensitive

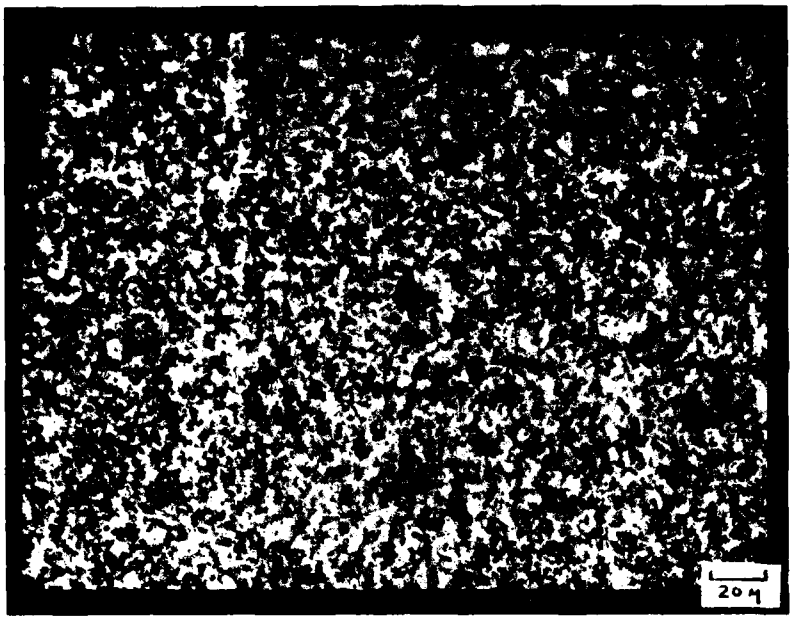

Reflected
Polarized
Light
400X

Crossed
Nicols
224X

FIGURE 20 - NC-132 Silicon nitride lapped surface - no treatment

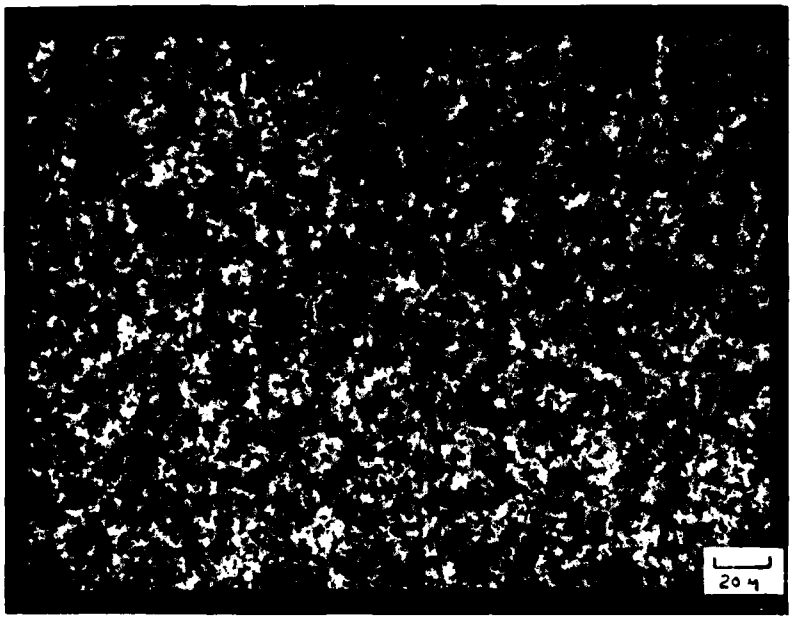

One hour
exposure
400X

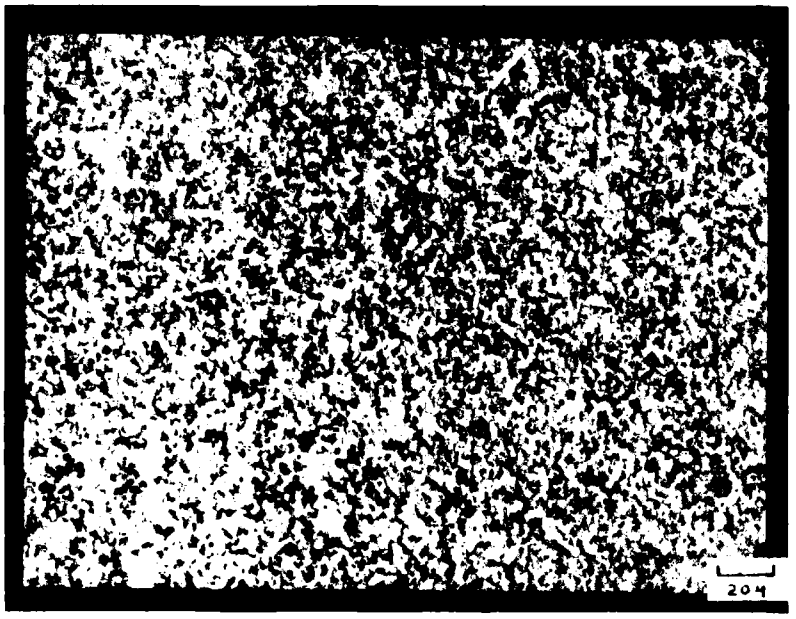

Two hour
exposure
400X

FIGURE 21 - NC-132 silicon nitride
600°C (1100°F) oxidation

One hour
exposure
400X

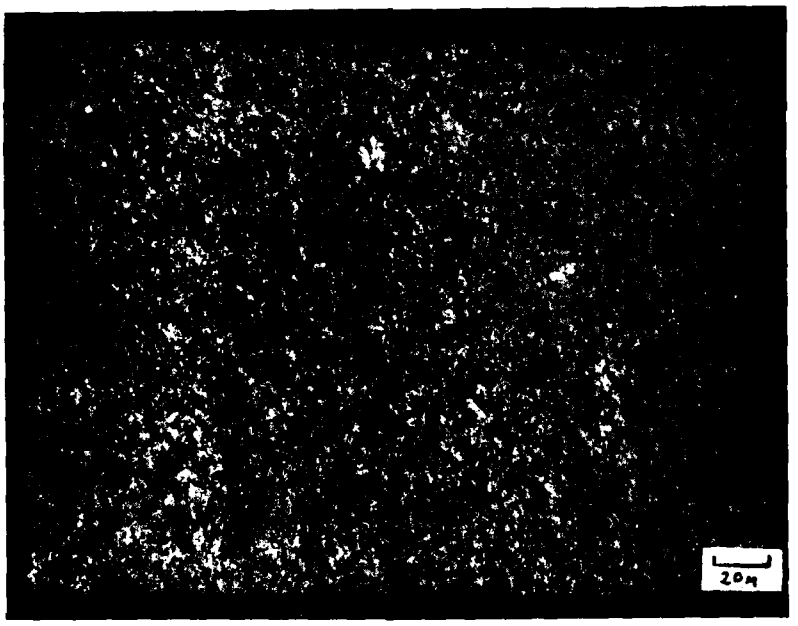

Two hour
exposure
400X

FIGURE 22 - NC-132 silicon nitride
750°C (1400°F) oxidation

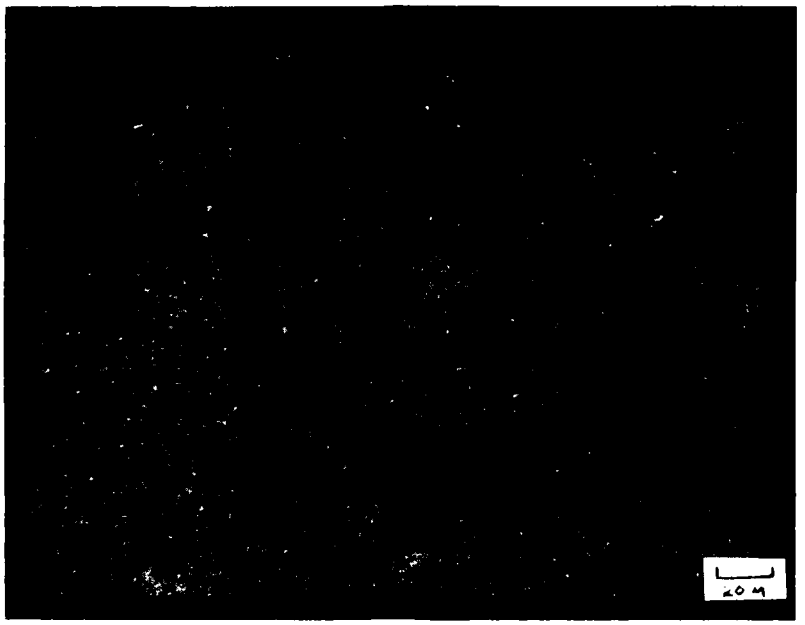

One hour
exposure
400X

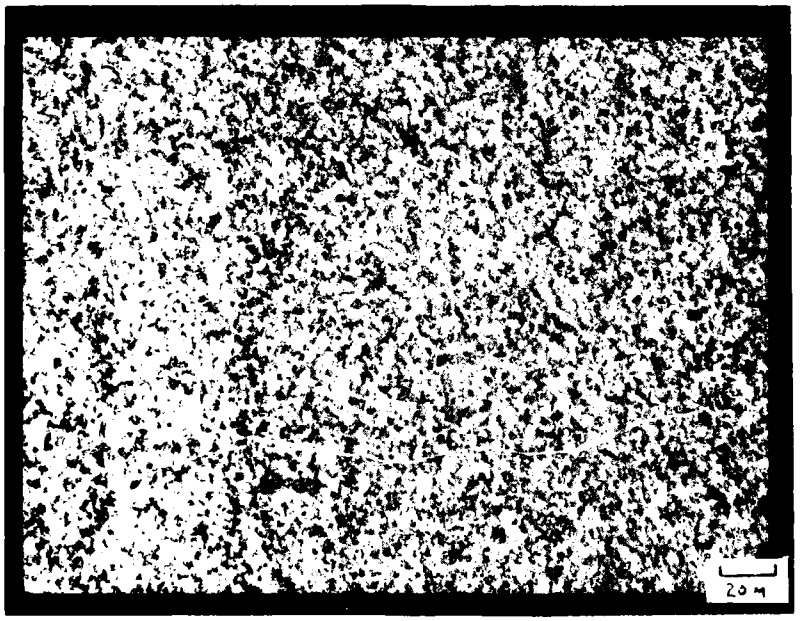

Two hour
exposure
400X

FIGURE 23 - NC-132 silicon nitride
900°C (1650°F) oxidation

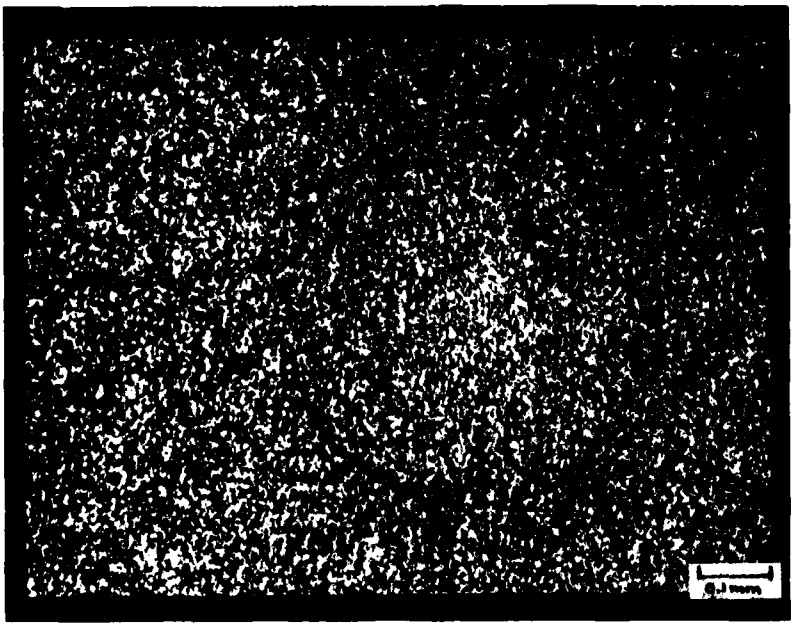

Lapped Surface
100X
Reflected Light

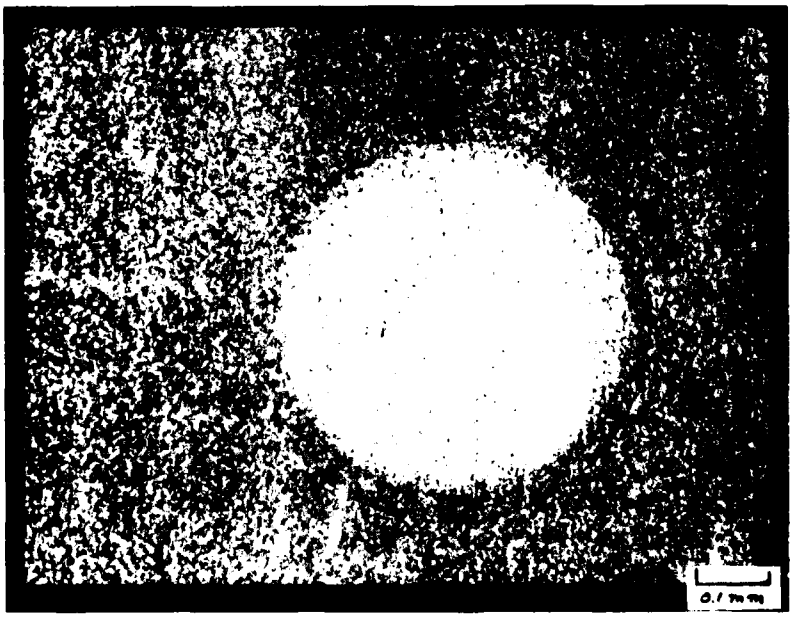

Lapped Surface
+ 1 hr @ 900°C
100X
Reflected Light

FIGURE 24 - NC-132 silicon nitride
Hertzian cone cracks

Lapped Surface
100X
Dark Field

Lapped Surface
+ 1 hr @ 900°C
100X
Dark Field

FIGURE 25 - NC-132 silicon nitride
Hertzian cone cracks

to specular surface reflection. The light path is parallel to the sample surface until reflected into the microscope ocular. Flat, smooth areas will appear darker than rough ones. Figure 25 shows that the only real change in surface topography is at the crack itself in the as-lapped surface. The oxidized surface has a smoother surface in the compressive zone in addition to the cone crack. Figure 26 illustrates the appearance of the same oxidized crack, as discussed above under crossed Nicols. As discussed earlier, light areas in a nearly extinct field are probably lower density areas that allow more light to enter and reflect in a different orientation to pass through the analyzer. A crack re-orients polarized light by reflecting it off the two fracture surfaces. Thus, the cone crack is clearly seen. The lack of reflectivity in the compressive contact zone shows that the failure there is of a much finer scale than at the cone crack itself.

Figures 27 and 28 are secondary emmission electron micrographs of the cone crack/specimen surface intersection. The crack is lighter in tone due to local charging. The surface of the NC-132 in Figure 27 is typical of a carefully finished specimen; the microstructure of the material is fairly apparent with details of less than 2u m. The irregularities in the crack front (saw-tooth effect) are, in size, the same general scale as the grain size. Figure 28 shows a typical surface morphology of a lightly oxidized NC-132 silicon nitride surface. The crack front's

Lapped Surface
+ 1 hr @ 900°C

Crossed Nicols

FIGURE 26 - NC-132 silicon nitride Hertzian cone crack

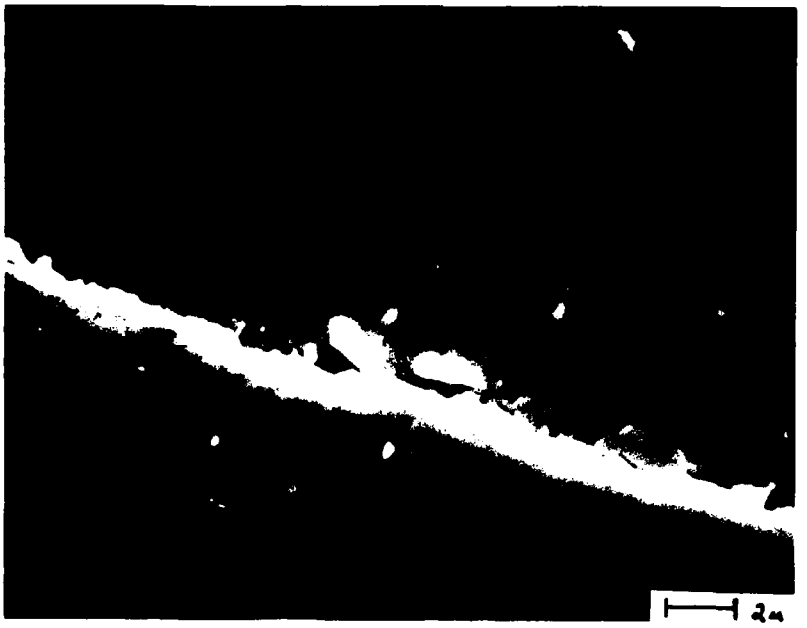

FIGURE 27 - Hertzian crack morphology lapped surface

FIGURE 28 - Hertzian crack morphology NC-132
2 hours @ 900°C (1650°F)

appearance is considerably different -- strongly resembling a coplanar tensile fracture of mica sheet type minerals. Here, tensile crack propogation appears to have been resisted by the formation of thin oxidation films.

The results of the indentation study are presented in Table I. Where surface distress was evident, it was found that the measured contact radius agreed with the calculated radius within 5 percent. The oxidation treatments at 900°C increased the stress required for tensile failure by an amount that is statistically significant. As noted earlier, however, the durability of this oxidized surface under cyclic Hertzian stress is in question.

This increase of approximately 5 percent in the average fracture load does indicate potential for increasing the rolling contact fatigue life up to 15 percent. If the oxidation film is securely anchored to the silicon nitride substrate and can be ground off, leaving "blunted" surface flaws; both the compressive and tensile strength advantages of pure and oxidized silicon nitride surfaces, respectively may be maintained. The potential of oxide films as a solid lubricant is also of interest.

E. Conclusions

Improvement of NC-132 silicon nitride behavior by either stuffed silicon nitride derivatives or oxidized surface flaws is still feasible. Future efforts should include looking at less active ion exchange media for chemical tempering or possibly molten salt transfer. A more complete characterization of the oxidation film's adherance and depth is called for. If the film's compressive strength degradation can be negated, perhaps by a final lapping operation, performance of the NC-132 silicon nitride in a rolling contact bearing environment may be measureably improved.

TABLE I

STATIC HERTZIAN LOADING - FRACTURE INITIATION
NC-132 Silicon Nitride/Tungsten Carbide Indenter

Treatment	Average Compressive Stress* @ Fracture/ Std. Dev. GN/m^2	Compressive Stress -2 Std. Dev. GN/m^2	Maximum Tensile Stress @ Fracture/ Std. Dev. GN/m^2	Tensile Stress -2 Std. Dev. GN/m^2	Number of Samples
None	8.69	8.07	2.18	2.01	52
1 hr @ 600°C	8.62	7.10	2.16	1.78	33
2 hr @ 600°C	8.41	5.79	2.10	1.45	35
1 hr @ 750°C	8.83	7.86	2.21	1.98	54
2 hr @ 750°C	8.83	8.07	2.21	2.02	32
1 hr @ 900°C	8.96	7.72	2.25	1.93	33
2 hr @ 900°C	9.17	8.27	2.29	2.07	33

*Load/πa^2; a = contact radius

REFERENCES

1. Hamburg, et.al., "Ceramic Roller Bearings - J402 Engine," Final Report, NASC Contract N00140-76-C-1104, 1979.

2. Dala, H. M., "Development of Basic Processing Technology for Bearing Quality Silicon Nitride Balls," Final Report, NASC Contract N00019-76-C-0684, (1977).

3. Weaver, G. Q. and Lucek J. W., "Optimization of Si_3N_4-Y_2O_3 Hot Pressed Materials", Bull. Am. Ceram. Soc. 57-12 (1978) 1131.

4. Lucek, J. W. and Cowley, P. E., "Investigation of the Use of Ceramics in Aircraft Engine Bearings", Final Report, Naval Air Systems Command Contract N00019-76-C-0251, (1979).

5. Dalal, et.al., "Effect of Lapping Parameters on the Generation of Damage on Silicon Nitride Ball Surfaces", Final Report NASC Contract N00019-76-C-0147, (1976).

6. Sibley, L. B., et al, "A Laboratory Evaluation of Some Ceramic and Cermet Materials for Bearing and Seal Applications in Aircraft Auxiliary Power Units and Liquid Rocket Motors", WADC TR 57-4 (1956).

7. Wilson, D. C. Gray, S., Sibley, L. B., et al, "The Development of Lubricants for High-Speed Rolling Contact Bearings Operating at 1200°F Temperature", WADC TR 59-790 (1959).

8. Cosgrove, S. L. Sibley, L. B. and Allen, C. M., "Evaluation of Dry Powdered Lubricants at 1000°F in a Modified Four-Ball-Wear Machine", ASLE Trans., 2 (2), 217-224 (1960).

9. Sibley, L. B. and Allen, C. M., "Friction and Wear Behavior of Refractory Materials at High Sliding Velocities and Temperatures", Wear, 5, 312 (1962).

10. Taylor, K. M., Sibley, L. B. and Lawrence, J. C., "Development of a Ceramic Rolling Contact Bearing for High Temperature Use", Wear, 6, 226-240 (1963).

11. Campbell, M. E., and Thompson, M. B., "Lubrication Handbook for Use in the Space Industry, Part A - Solid Lubricants", NASA Marshall Space Flight Center Contract NAS8-27662 (1972).

12. Lipp, L. C., Van Wyk, J. W. and Williams, F. J., "Development of Solid Lubricant Compact Bearings for the Supersonic Transport", Lubrication Engineering 29 (3) 108-115 (1973).

13. Archard, J. F., and Hirst, W., "The Wear of Metals Under Unlubricated Conditions:, Proc. Roy. Soc., Series A, 236, 397140 (1956).

14. Tallian, T. E., McCool, J. I., and Sibley, L. B., "Partial Elastohydrodynamic Lubrication of Rolling Contacts", Symposium on Elastohydrodynamic Lubrication, Paper No. 14, Inst. Mech. Engrs., London (1965).

15. Baumgartner, H. R., and Richerson, D. W., "Inclusion Effects on the Strength of Hot Pressed Si_3N_4", Fracture Mechanics of Ceramics, Vol. 1, Concepts, Flaws and Fractography, Plenum Press, New York, pp. 367-386 (1974).

16. Handbook of Chemistry and Physics; The Cehmical Rubber Handbook, 1971.

17. Searcy, et.al., Chemical and Mechanical Behavior of Inorganic Materials, Wiley Interscience, New York, 1970, pp 33ff.

18. AiResearch Manufacturing Company of Arizona, Ceramic Gas Turbine Demonstration Program, Interim Report Number 4, Section 4 March 1977.

19. Wilshaw, T. R., J. Physics D. Appl. Phys., 4 (1971) 1567.

20. Langitan, F. B. and Lawn, B. R., J. Appl. Physics, 41 (1970) 3357.

21. Swindlehurst and Wilshaw, J. Mat. Science; 11 (1963) 1653.

APPENDIX A

COMPRESSIVE STRENGTH DETERMINATION FOR HIGH STRENGTH CERAMIC MATERIALS

Appl. Documents - ASTM Specification C773-74

Modifications to noted specification to allow testing of very strong materials occur as noted below.

7.3 Contact Cylinders - substitute tungsten carbide contacts to be reground when damaged. Also incorporate 0.001 inch thick soft aluminum foil as cushion pads (4.4 modified).

8.1 Preparation - as specified with the following additions:

a. Rough grind cylinders with 100 grit or finer diamond wheel at 0.0005"/pass stock removal maximum.

b. Slice to length with 150 grit diamond

c. Finish all over with 320 grit diamond at 0.00025"/pass maximum stock removal rate with 0.003" stock to be removed in this step (minimum).

APPENDIX B

Talysurf Traces of Various Test Tracks

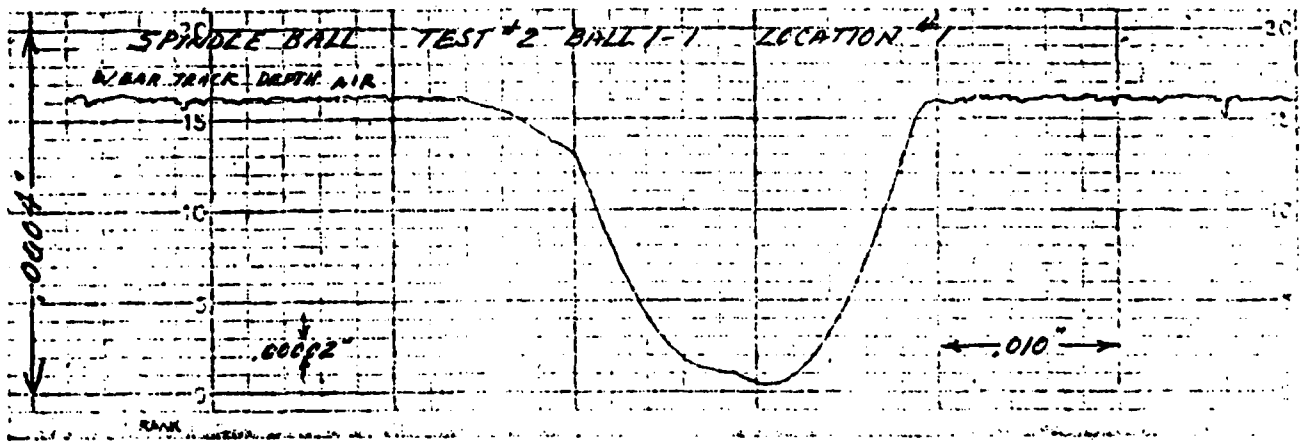

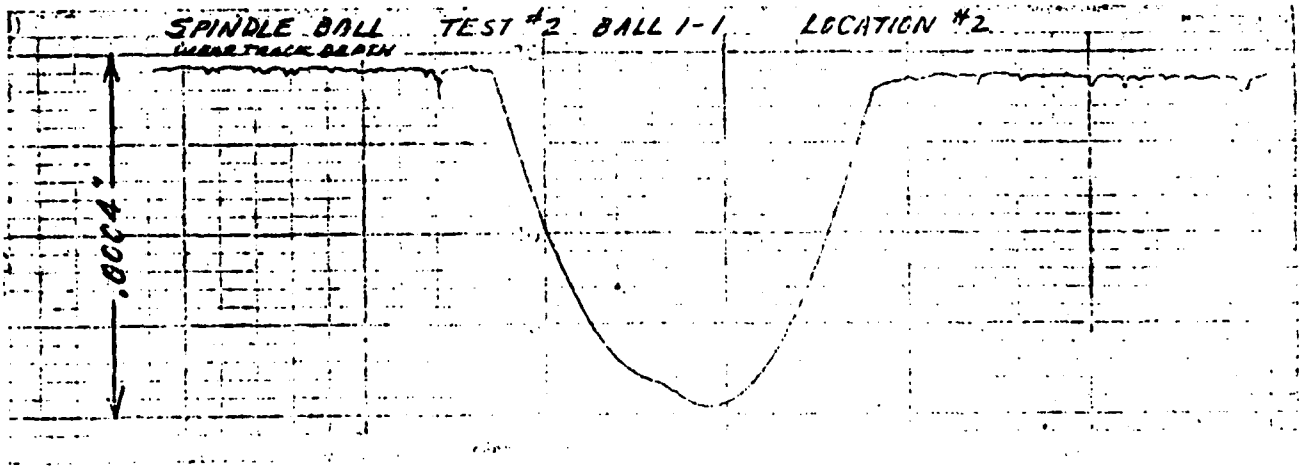

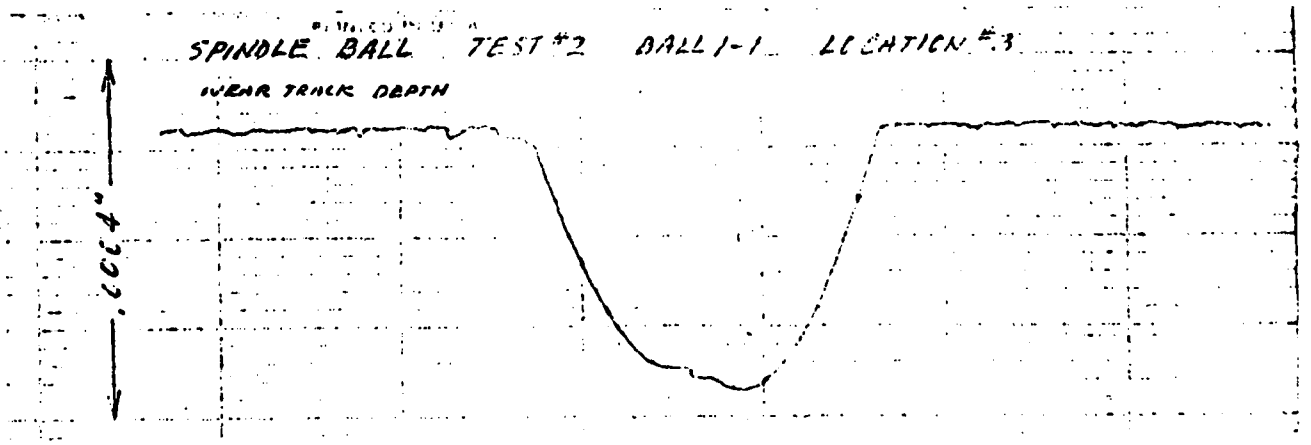

Talysurf Traces at Three Locations on Wear Track, Test 1-1, Uncoated.

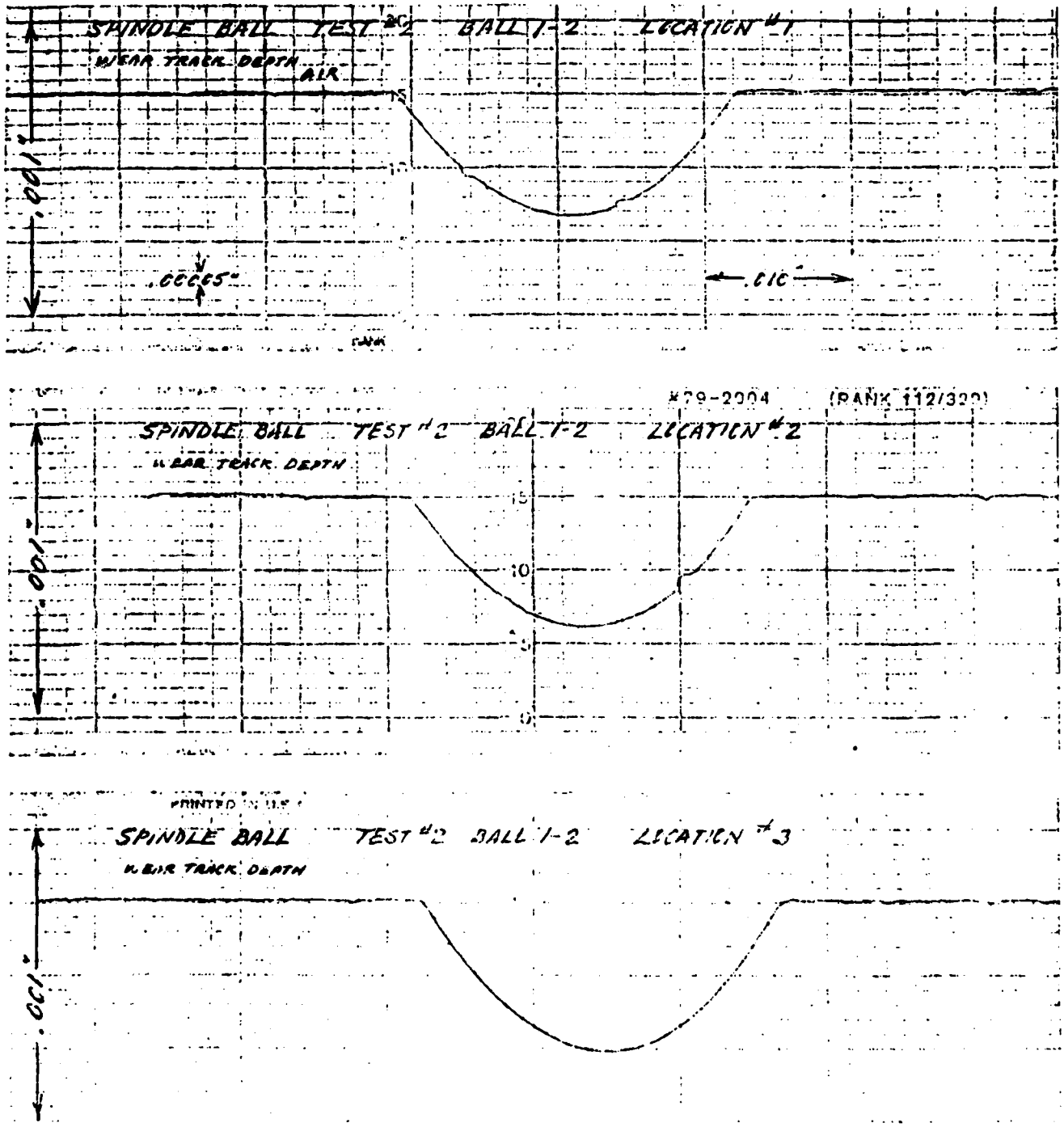

Talysurf Traces at Three Locations on Wear Track, Test 1-2, Uncoated.

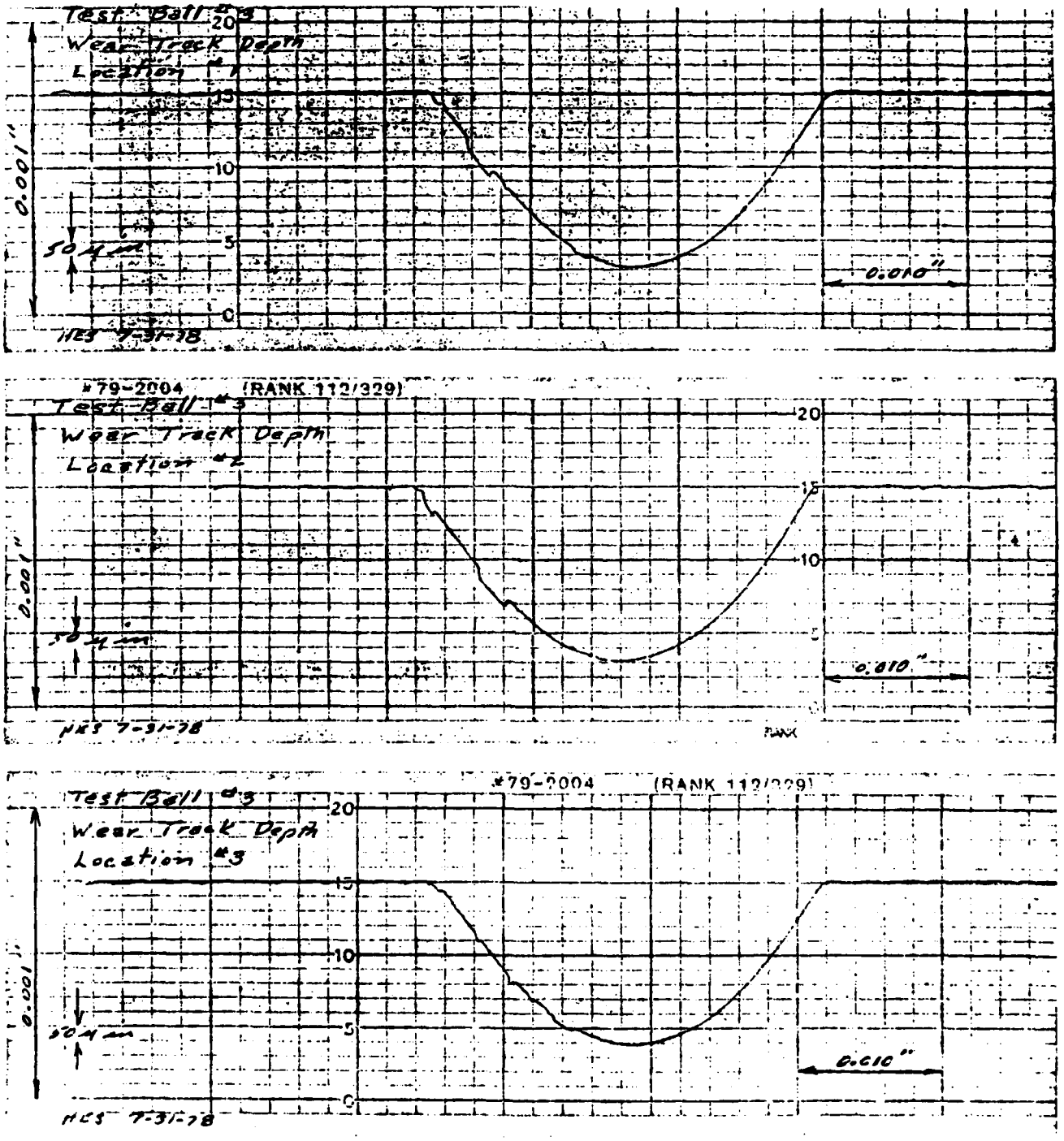

Talysurf Traces at Three Locations on Wear Track, Test 2-1, with Vitrolube Coating.

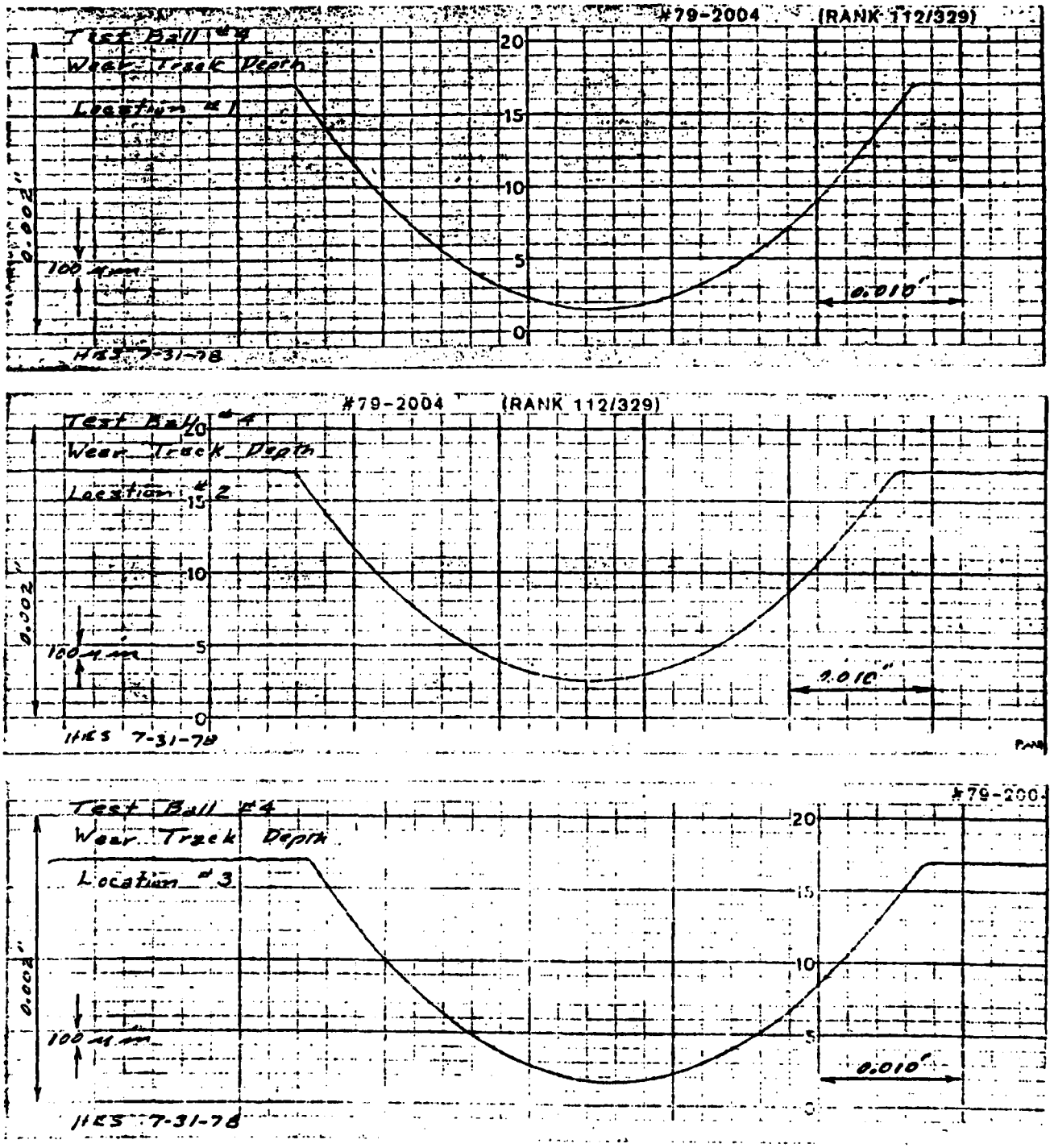

Talysurf Traces at Three Locations on Wear Track, Test 2-2, with Vitrolube Coating.

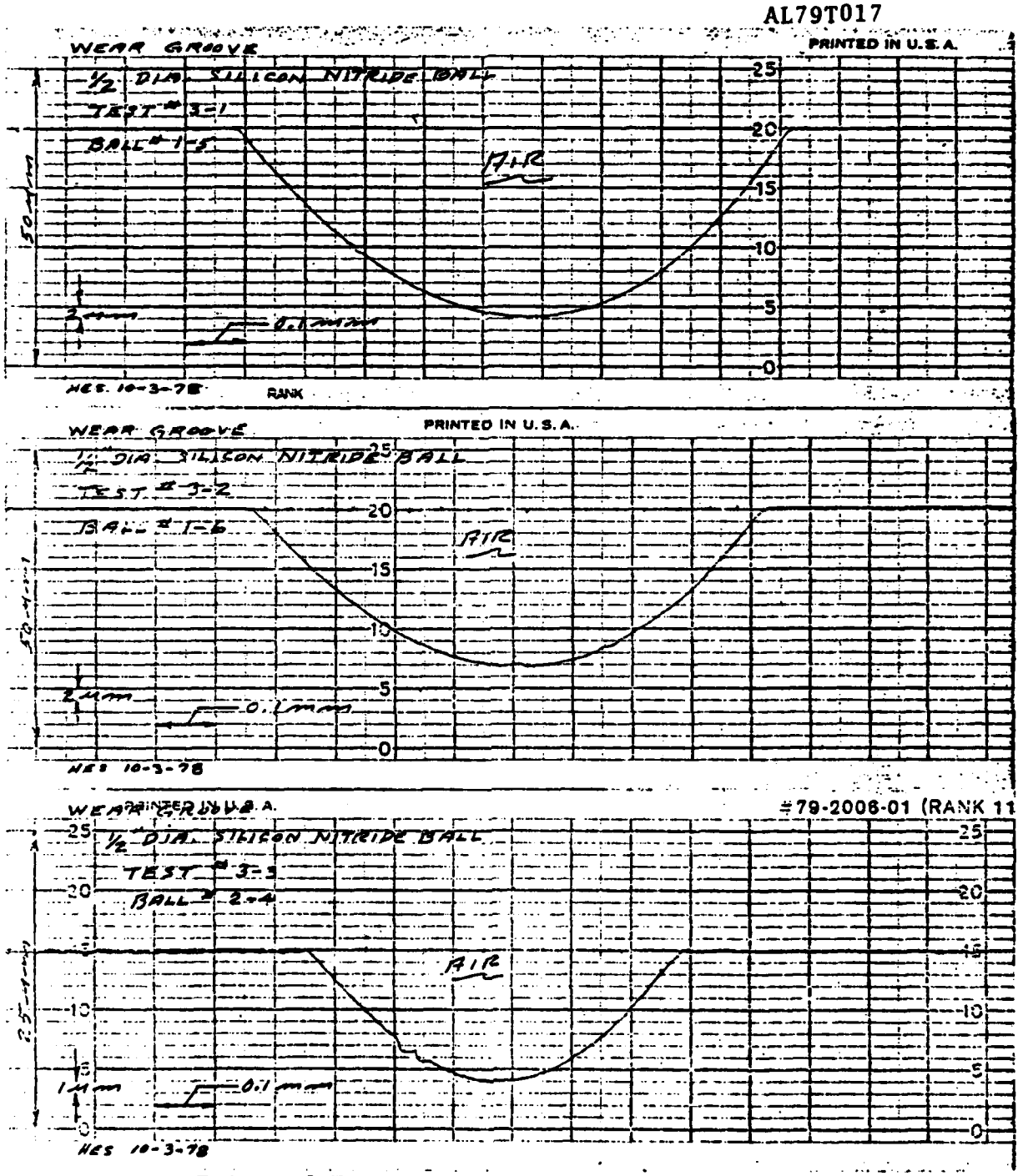

Talysurf Traces on Wear Tracks with Sputter Coated MoS_2, Tests 3-1, 3-2 and 3-3

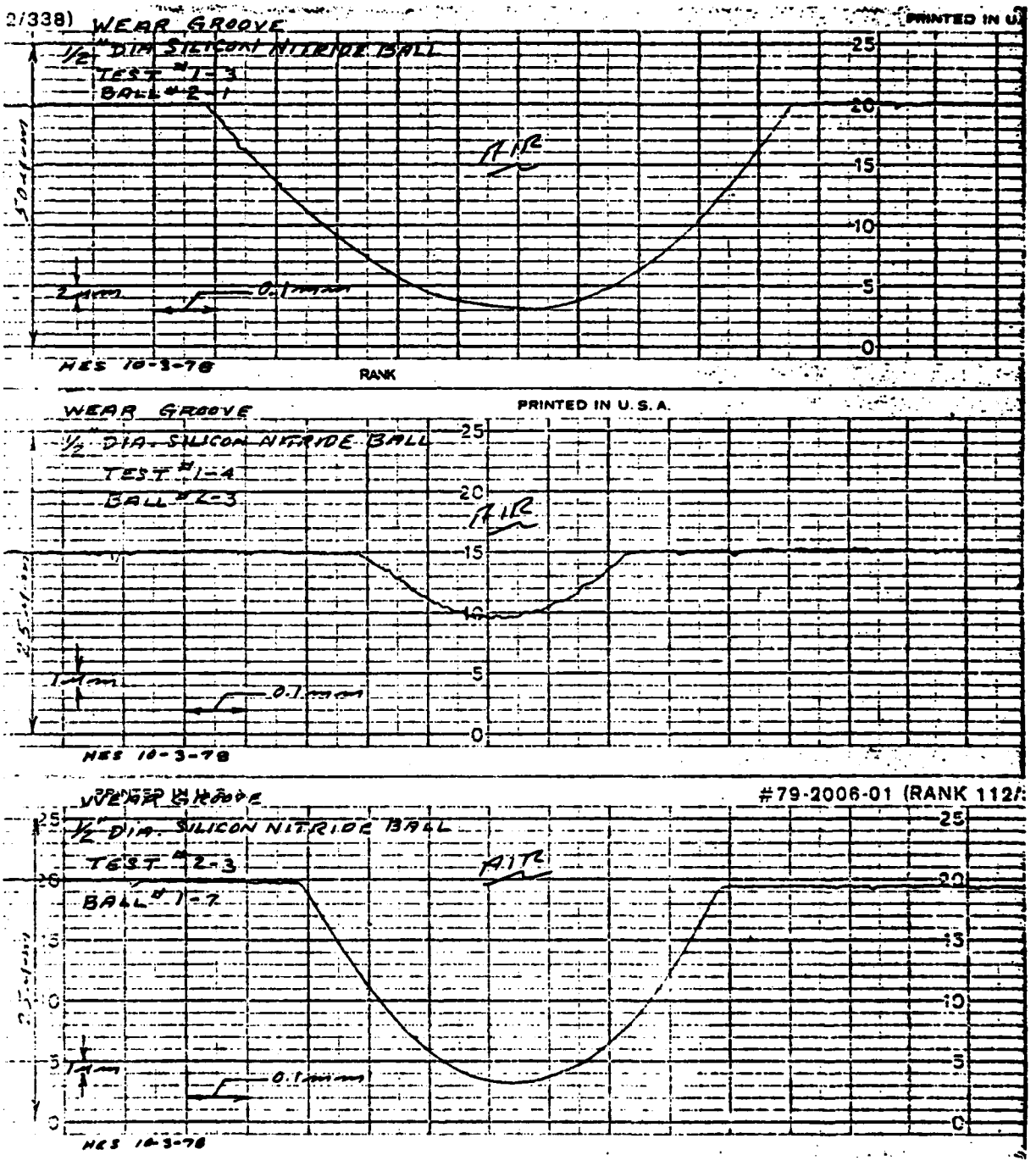

Talysurf Traces on Wear Tracks Uncoated and with Vitrolube Coating, Tests 1-3, 1-4 and 2-3

APPENDIX C

BIBLIOGRAPHY

Carter, T. L., and Zaretsky, E. V., "Rolling Contact Fatigue Life of a Crystallized Glass Ceramic", NASA TN D-259 (1960).

Zaretsky, E. V. and Anderson, W. J. "Rolling Contact Fatigue Studies with Four Tool Steels and Crystallized Glass Ceramic", J. Basic Eng., Trans. ASME, Series D, 83, 1961, 603.

Taylor, K. M., Sibley, L. B. and Lawrence, J. C., "Development of a Ceramic Rolling Contact Bearing for High Temperature Use". ASME 61 Lubs-12 (1961).

Bamberger and Baughman, "Unlubricated High Temperature Bearing Studies", J. Bas. Eng. 6:63, p 265.

Swindlehurst, W. E. and Wilshaw, I. R., J. Mat. Science, 11 (1963) 1653.

Appledoorn, J. K., and Royle, R. C., "Lubricant Fatique Testing with Ceramic Balls", J. ASLE 2, 45 (1965).

Parker, R. J. Grisaffe, S. G. and Zaretsky, E. V., "Rolling Contact Studies with Four Refractory Materials to 2000°F", ASLE Trans., 8, 1965, 208.

Langitan, F. B. and Lawn, B. R., J. Appl. Phys., 41 (1970) 3357.

Scott, D., Blackwell, J., and McCullagh, P. J., "Silicon Nitride as a Rolling Bearing Material - A Preliminary Assessment", Wear 17, 73 (1971).

Wilshaw, T. R., J. Physics D. Appl. Phys. 4 (1971) 1567.

Schmitt, W. A. and Davey J. E., NBS Special Pub. 348, May 1972, p. 259.

Hockey, B. J., in NBS Special Pub. 348, May 1972, p. 333.

Wachtman, J. B. Capps, W. and Mandel, J., "Biaxial Flexure Tests of Ceramic Substrates," J. Matls. 7, 188 (1972).

Parker, R. J., and Zaretsky, E. V., "Rolling Element Fatigue Life of Silicon Nitride Balls - Preliminary Test Results, NASA TMZ-68174 (1972).

Wheildon, W. M., Baumgartner, H. R., Sundberg, D. V., and M. L. Torti "Ceramic Materials in Rolling Contact Bearings", Final Technical Report under NASC Contract N00019-72-C-0299, 1973.

Baumgartner, H. R. and Richerson, R. W., "Inclusion Effects on the Strength of Hot Pressed Silicon Nitride," in Fracture Mechanics of Ceramics, pp. 367, Plenum (1973).

Baumgartner, H. R. and Wheildon, W. M., in Surfaces and Interfaces of Glass and Ceramics, V. B.Frechette, et.al. eds., Plenum Press, New York, 1973, p. 179.

Baumgartner, H. R., "Evaluation of Rolling Bearings Containing Hot-Pressed Silicon Nitride Rolling Elements", Second Army Materials Science Conference on Ceramics for High Performance Applications, Hyannis (1973)

Scott, D. and Blackwell, J.. "Hot Pressed Silicon Nitride as a Rolling Bearing Material - A Preliminary Assessment", Wear, 24, 61, (1973).

Baumgartner, H. R., Sundberg, D. V., and Wheildon, W. M., "Silicon Nitride in Rolling Contact Bearings", Final Report under NASC Contract N00019-73-C-0193.

Dalal, H., "Surface Interactions and Lubrication Response of Silicon Nitride Bearing Elements", Final Report under NASC Contract N00019-73-C-0193, 1973.

Valori, R., "Rolling Contact Fatigue of Silicon Nitride", Naval Air Propulsion Test Center Report No. NAPTC-PE-42, (August, 1974).

Evans, A. G. and Wiederhorn, S. M., J. Mat. Sci., 9, (1974), 270.

Parker, R. J. and Zaretsky, E. V., "Fatigue Life of High-Speed Ball Bearings with Silicon Nitride Balls", J. Lub. Tech., Trans. ASME, Series F, 97, 1975.

Baumgartner, H. R., and Cowley, P. E., "Silicon Nitride in Rolling Contact Bearings", Final Report under NASC Contract N00019-74-C-0157, 1975.

Baumgartner, H. R., and Cowley, P. E., "Finishing Techniques for Silicon Nitride Bearings", Final Report No. AMMRC CTR 76-5 on Contract DAAG46-74-C-0055 (March 1976).

Dalal, H. M., et al, "Effect of Surface and Mechanical Properties on Silicon Nitride Bearing Element Performance", SKF Report No. AL75T002, Final Report on Naval Air Systems Command Contract N00019-74-C-0168 (February, 1975).

Derkacs, T., et al, "Non-Destructive Evaluation of Ceramics," Final Report on Naval Air Development Center Contract No. N00019-75-C-0238, (July 1976).

Reddecliff, J. M., "Silicon Nitride Ball Bearing Demonstration Test", Pratt & Whitney Aircraft Report No. FR-6995, Final Report on NAPTC Contract N00140-75-C-0382 (May 1975).

Huerta, M. and Malkin, S., "Grinding of Glass: Surface Structure and Fracture Strength", ASME Proceedings, General Engineering Conference, Paper No. 75-Prod. 2 (May 1975).

Reddecliff, J. M. and Valori, R., "The Performance of a High-Speed Ball Thrust Bearing Using Silicon Nitride Balls, Paper No. 76-LubS-8 presented at the ASME Lubrication Symposium, Atlanta, GA., May 24-26, 1976.

Dalal, H. M., et al, "Effect of Lapping Parameters on Generation of Damage on Silicon Nitride Ball Surfaces", SKF Report No. AL76T026, Final Report on U. S. Department of the Navy Contract No. N00019-76-C-0147 (December, 1976).

Rowcliffe, D. J. and Jorgensen, P. J., "Sintering of Silicon Nitride," Proceedings: Workshop on Ceramics for Advanced Heat Engines, sponsored by ERDA, pp. 191, Orlando, Florida, (1977).

Dalal, H. M., et al, "Development of Basic Processing Techology for Bearing Quality Silicon Nitride Balls", SKF Reports AL77T012, AL77T026 and AL77T040, Quarterly Reports Nos. 1-3 on U. S Deaprtment of the Navy Contract No. N00019-76-C-0684 (1977).

Derkacs, T., et al, "Ultrasonic Inspection of Ceramics Containing Small Flaws", Final Report on Naval Air Development Center Contract No. N62269-76-C-0948, March, (1977).

Weaver, G. Q., and Lucek, J. W., "Optimization of Si_3N_4-Y_2O_3 Hot Pressed Materials", Bull. Am. Ceram. Soc. 57-12 (1978) 1131.

Hamburg, et.al., Final Report on Contract N00140-76-C-1104.

DISTRIBUTION LIST

	No. of Copies
Naval Air Systems Command Washington, D.C. 20361 Attention: AIR 950D 9 310C 1 330 1 536 1 5163D4 6	18
Office of Naval Research Washington, D.C. 20360 Attention: Code 471	1
White Oak Laboratory Naval Surface Weapons Center White Oak, Maryland 20910 Attention: Code 2301	1
Naval Research Laboratory Washington, D.C. 20390 Attention: Code 6360	1
David W. Taylor Naval Ship Research & Development Center Annapolis, Maryland 21402 Attention: W. Smith, Code 2832	1
Naval Air Propulsion Center Trenton, New Jersey 08628 Attention: R. Valori, Code PE 72	1
Naval Undersea Center San Diego, California 92132 Attention: Dr. J. Stachiw	1
Naval Air Development Center Materials Application Branch, Code 6061 Warminster, Pennsylvania 18974	1
Air Force Materials Laboratory Wright-Patterson Air Force Base Dayton, Ohio 45433 Attention: Dr. H. Graham, LLM 1 Dr. R. Rah, LLM 1 Dr. P. Land, LPJ 1 Lt. B. Togge, LTM 1	4
Air Force Aero Propulsion Laboratory Wright-Patterson Air Force Base, Ohio 45433 Attention: Ron Dayton (SFL)	1

	No. of Copies
Director Applied Technology Laboratory U.S. Army Research & Technology Laboratories Fort Eustis, Virginia 23604 Attention: DAVDL-ATL-ATP (Mr. Pauze)	1
U.S. Army Research Office Box CM, Duke Station Durham, North Carolina 27706 Attention: CRDARD	1
U.S. Army MERDC Fort Belvoir, Virginia 22060 Attention: W. McGovern (SMEFB-EP)	1
Army Materials and Mechanics Research Center Watertown, Massachusetts 02172 Attention: Dr. R. N. Katz	1
NASA Headquarters Washington, D.C. 20546 Attention: J. J. Gangler, RRM	1
NASA Lewis Research Center 21000 Brookpark Road Cleveland, Ohio 44135 Attention: Dr. E. Zaretsky 1 W. A. Sanders (49-1) 1 and Dr. T. Hergell	2
Defense Advanced Research Project Office 1400 Weilson Boulevard Arlington, Virginia 22209 Attention: Dr. Van Reuth 1 Mr. Buckley 1	2
Inorganic Materials Division Institute for Materials Research National Bureau of Standards Washington, D.C. 20234	1
University of California Lawrence Berkeley Laboratory Hearst Mining Building Berkeley, California 94720 Attention: Dr. L. Froschauer	1

	No. of Copies
Department of Engineering University of California Los Angeles, California 90024 Attention: Profs. J. W. Knapp and G. Sines	1
Department of Metallurgy Case-Western Reserve University Cleveland, Ohio 44106 Attention: Dr. A. Heuer	1
Engineering Experiment Station Georgia Institute of Technology Atlanta, Georgia 30332 Attention: J. D. Walton	1
Department of Engineering Research North Carolina State University Raleigh, North Carolina 27607 Attention: Dr. H. Palmour	1
Materials Research Laboratory Pennsylvania State University University Park, Pennsylvania 16802 Attention: Prof. Rustum Roy	1
Rensselaer Polytechnic Institute 110 Eighth Street Troy, New York 12181 Attention: R. J. Diefendorf	1
School of Ceramics Rutgers, The State University New Brunswick, New Jersey 08903	1
Virginia Polytechnic Institute Minerals Engineering Blacksburg, Virginia 24060 Attention: Dr. D. P. H. Hasselman	1
Aerospace Corporation Materials Laboratory P.O. Box 95085 Los Angeles, California 90045	1
Supervisor, Materials Engineering Department 93-39M AiResearch Manufacturing Company of Arizona 402 South 36th Street Phoenix, Arizona 85034	1

	No. of Copies
Materials Development Center AVCO System Division Wilmington, Massachusetts 01887 Attention: Tom Vasilos	1
Lycoming Division AVCO Corporation Stratford, Connecticut 06497 Attention: Mr. D. Wilson	1
Barden Corporation Danbury, Connecticut 06810 Attention: Mr. K. MacKenzie	1
Batelle Memorial Institute Ceramics Department 505 King Avenue Columbus, Ohio 43201	1
Metals and Ceramics Information Center Batelle Memorial Institute 505 King Avenue Columbus, Ohio 43201	1
Bell Helicopter Textron P.O. Box 482 Fort Worth, Texas 76101 Attention: R. Battles	1
The Boeing Company Materials and Processes Laboratories Aerospace Group P.O. Box 3999 Seattle, Washington 98124	1
Research and Development Division Carborundum Company Niagara Falls, New York 14302 Attention: Mr. C. McMurty	1
Caterpillar Tractor Company Technical Center East Peoria, Illinois 61611 Attention: A. R. Canady	1
Ceramic Finishing Company Box 498 State College, Pennsylvania 16801	1
Ceradyne Inc. Box 1103 Santa Ana, California 92705	1

	No. of Copies
Coors Porcelain Company 600 Ninth Street Golden, Colorado 80401 Attention: Research Department	1
Cummings Engine Company Columbus, Indiana 47201 Attention: Mr. R. Kamo, Director of Research	1
Curtiss-Wright Company Wright Aeronautical Division One Passaic Street Wood-Ridge, New Jersey 07075	1
Fafnir Bearing Company Division Textron Corporation 27 Booth Street New Britain, Connecticut 06050	1
F.A.G. Bearing Corporation 70 Hamilton Avenue Stamford, Connecticut 06904 Attention: Joseph Hoo	1
Federal-Mogul Corporation Anti-Friction Bearing R&D Center 3980 Research Park Drive Ann Arbor, Michigan 48104 Attention: D. Glover	1
Product Development Group Ford Motor Company 20000 Rotunda Drive Dearborn, Michigan 28121 Attention: Mr. E. Fisher	1
Aircraft Engine Group Technical Information Center Main Drop N-32, Building 700 General Electric Company Cincinnati, Ohio 45215	1
Metallurgy and Ceramics Research Department General Electric R&D Laboratories P.O. Box 8 Schenectady, New York 12301	1
Space Sciences Laboratory General Electric Company P.O. Box 8555 Philadelphia, Pennsylvania 19101	1

	No. of Copies
Detroit Diesel Allison Division General Motors Corporation P.O. Box 894 Indianapolis, Indiana 46206 Attention: Dr. M. Herman	1
NDH Division General Motors Corporation Hayes Street Sandusky, Ohio Attention: H. Woerhle	1
Hughes Aircraft Company Aerospace Group R&D Division Culver City, California 90130	1
IIT Research Institute 10 West 35th Street Chicago, Illinois 60616 Attention: Ceramics Division	1
Industrial Tectonics, Inc. 18301 Santa Fe Avenue Compton, California 90224 Attention: Hans R. Signer	1
Kaweki-Berylco Industry Box 1462 Reading, Pennsylvania 19603 Attention: Mr. R. J. Longnecker	1
Research and Development Division Arthur D. Little Company Acorn Park Cambridge, Massachusetts 02140	1
Mechanical Technology, Inc. 968 Albany-Shaker Road Latham, New York 12110 Attention: Dr. E. F. Finkin	1
North American Rockwell Science Center P.O. Box 1085 Thousand Oaks, California 91360	1
Rollway Bearing Company Division Lipe Corporation 7600 Morgan Road Liverpool, New York 13088 Attention: B. Dalton	1

	No. of Copies
Ceramic Division Sandia Corporation Albuquerque, New Mexico 87101	1
Engineering and Research Center SKF Industries, Inc. 1100 First Avenue King of Prussia, Pennsylvania 19406 Attention: L. Sibley	1
Solar Division International Harvester Company 2200 Pacific Highway San Diego, California 92112 Attention: Dr. A. G. Metcalfe	1
Southwest Research Institute P.O. Drawer 28510 San Antonio, Texas 78228	1
Materials Sciences & Engineering Laboratory Stanford Research Institute Menlo Park, California 84025 Attention: Dr. Cubiciotti	1
Teledyne CAE 1330 Laskey Road Toledo, Ohio 43601 Attention: R. Beck	1
The Tinken Company Canton, Ohio 44706 Attention: R. Cornish	1
Marlin Rockwell, Division of TRW Jamestown, New York 14701 Attention: John C. Lawrence and A. S. Irwin	1
Union Carbide Corporation Parma Technical Center P.O. Box 6116 Cleveland, Ohio 44101	1
Materials Sciences Laboratory United Aircraft Corporation East Hartford, Connecticut 06101 Attention: Dr. J. J. Brennan	1

	No. of Copies
Pratt & Whitney Aircraft Division United Aircraft Corporation East Hartford, Connecticut 06108 Attention: Paul Brown EB-2	1
Pratt & Whitney Aircraft Division United Aircraft Corporation Middletown, Connecticut 06108 Attention: L. E. Friedrich, MERL	1
Pratt & Whitney Aircraft Division United Aircraft Corporation Florida R&D Center West Palm Beach, Florida Attention: Mr. J. Miner	1
Astronuclear Laboratory Westinghouse Electric Corporation Box 10864 Pittsburg, Pennsylvania 15236	1
Westinghouse Research Laboratories Beulah Road Churchill Borough Pittsburgh, Pennsylvania 15235 Attention: Dr. R. Bratton	1
Williams Research Corporation Walled Lake, Michigan 48088	1
Litton Guidance & Control Systems 5500 Canoga Ave Woodland Hills, CA 91364 ATTN: Robert A. Westerholm, Mail Station 87	1
Officer in Charge of Construction Civil Engineering Laboratory Naval Facility Engineering Command Detachment Naval Construction Battalion Center Port Hueneme, CA 93043 ATTN: Stan Black, Code L40	1